JGR Biogeosciences

RESEARCH ARTICLE
10.1029/2024JG008147

The Validity of Optical Properties as Tracers of Terrigenous Dissolved Organic Carbon During Extensive Remineralization in Coastal Waters

Yuan Chen[1], **Yongli Zhou**[1,2], **and Patrick Martin**[1]

[1]Asian School of the Environment, Nanyang Technological University, Singapore, Singapore, [2]Now at Department of Geography, University of Hong Kong, Hong Kong, China

Key Points:

- Chromophoric dissolved organic matter removal was more than terrestrial dissolved organic carbon (tDOC) remineralization in coastal water
- Commonly used optical properties can quantify percent tDOC in natural environment but with different sensitivity
- Optical properties do not clearly indicate the extent of tDOC remineralization from complex natural biogeochemical processing

Supporting Information:

Supporting Information may be found in the online version of this article.

Correspondence to:

Y. Chen and P. Martin,
yuan006@e.ntu.edu.sg;
pmartin@ntu.edu.sg

Citation:

Chen, Y., Zhou, Y., & Martin, P. (2024). The validity of optical properties as tracers of terrigenous dissolved organic carbon during extensive remineralization in coastal waters. *Journal of Geophysical Research: Biogeosciences*, *129*, e2024JG008147. https://doi.org/10.1029/2024JG008147

Received 18 MAR 2024
Accepted 15 AUG 2024

Author Contributions:

Conceptualization: Patrick Martin
Data curation: Yuan Chen, Patrick Martin
Formal analysis: Yuan Chen, Yongli Zhou
Funding acquisition: Patrick Martin
Investigation: Yuan Chen
Methodology: Yuan Chen, Yongli Zhou
Project administration: Patrick Martin
Software: Yuan Chen
Supervision: Patrick Martin
Validation: Yuan Chen
Visualization: Yuan Chen
Writing – original draft: Yuan Chen
Writing – review & editing: Yuan Chen, Yongli Zhou, Patrick Martin

Abstract Terrestrial dissolved organic carbon (tDOC) is significant for coastal carbon cycling, and spectroscopy of chromophoric and fluorescent dissolved organic matter (CDOM, FDOM) is widely used to study tDOC cycling. However, CDOM and FDOM are often amongst the more labile components of tDOC. Because few studies have compared spectroscopy to measurements of both bulk tDOC concentration and tDOC remineralization, it remains unclear how accurately CDOM and FDOM actually trace tDOC in coastal waters when tDOC undergoes extensive remineralization. We collected a 4-year coastal timeseries in Southeast Asia, where tropical peatlands provide a large tDOC input. A carbon stable isotope mass balance shows that on average 53% of tDOC was remineralized upstream of our site, while 74% of CDOM was bleached. Despite this extensive tDOC remineralization and preferential CDOM loss, optical properties could still reliably quantify tDOC. CDOM spectral slope properties, such as $S_{275–295}$, are exponentially related to tDOC; these are highly sensitive tDOC tracers at low, but not at high, tDOC concentrations. Other properties are linearly related to tDOC, and both specific ultraviolet absorbance ($SUVA_{254}$) and DOC-normalized fluorescence intensity may be suitable to quantify tDOC over a wider range of concentrations. However, the optical properties did not show consistent changes with the extent of tDOC remineralization. Our data support the validity of CDOM and FDOM spectroscopy to trace tDOC across coastal gradients even after the majority of tDOC has been remineralized, but they also show that these measurements may not provide direct information about the degree of natural tDOC processing.

Plain Language Summary Dissolved organic carbon (DOC) derived from land plays an important role in coastal carbon cycling, which is widely studied using optical measurements. However, since there is a lack of environmental data sets that have measured optical properties together with both terrestrial DOC (tDOC) concentration and tDOC degradation, it remains unclear how accurately optical properties can quantify tDOC in coastal waters when tDOC is largely lost. In this study, we analyzed samples from coastal Southeast Asia and found that light-absorbing compositions of DOC is lost ~21% more than the total tDOC. Meanwhile, commonly used optical tDOC tracers all show ability of quantifying tDOC concentration but with different sensitivities. However, these optical properties may not reveal natural processing of tDOC quantitatively in coastal waters because of complex interactions of different processes.

1. Introduction

Annually around 0.25 Pg C of terrestrial dissolved organic carbon (tDOC) are transported from land to ocean, playing an important role in global and especially coastal carbon cycling (Ciais et al., 2013; Dai et al., 2012; Raymond & Spencer, 2015). A large fraction of tDOC is remineralized in ocean margin environments (Bélanger et al., 2006; Letscher et al., 2011; Painter et al., 2018). For instance, it is reported that 40%–70% of tDOC is remineralized on the Louisiana Shelf, in the Eurasian Arctic Shelf Sea and in the Sunda Shelf Sea before reaching the open ocean (Fichot & Benner, 2014; Kaiser et al., 2017; Zhou et al., 2021). The remineralization results in the formation of dissolved inorganic carbon (DIC) along with transformation of nutrient elements, thus lowering seawater pH (Capelle et al., 2020; Semiletov et al., 2016; Wit et al., 2018; Zhou et al., 2021) and influencing nutrient distributions (Alling et al., 2012; Qualls & Richardson, 2003; Vähätalo & Zepp, 2005). In addition, a fraction of tDOC—chromophoric dissolved organic matter (CDOM)—can absorb light, causing light attenuation in natural waters and affecting primary productivity and ecological functioning (Aksnes et al., 2009; Martin et al., 2021; Urtizberea et al., 2013).

Since terrestrial dissolved organic matter (tDOM) is rich in CDOM and fluorescent DOM (FDOM), absorbance and fluorescence spectroscopy are widely exploited to trace tDOC in aquatic environments, due to their high sensitivity and ease of measurement (Bauer & Bianchi, 2011; Coble, 2007; Dittmar, 2015; Stedmon & Nelson, 2015). The most commonly used optical properties (Table 1) include absorption coefficients (a_λ, m^{-1}), CDOM spectral slopes (such as $S_{275–295}$, nm^{-1}) and the CDOM spectral slope ratio ($S_R = S_{275–295}/S_{350–400}$), specific ultraviolet absorbance ($SUVA_{254}$, L mg-C^{-1} m^{-1}), the fluorescence index (FI) and the humification index (HIX). Typically, tDOC is characterized by higher values for a_λ, $SUVA_{254}$ and HIX, and lower values for $S_{275–295}$, S_R and FI, as compared to autochthonous DOC produced in aquatic environments (Gandois et al., 2014; Huguet et al., 2009; Kida et al., 2018; Stedmon et al., 2011). In addition, parallel factor analysis (PARAFAC) of FDOM spectra is commonly used to identify and quantify terrestrial fluorescent components to trace tDOC distribution in natural environments (Murphy et al., 2008; Stedmon et al., 2003). Apart from these indices of terrestrial source materials, the FDOM biological index (BIX) and more recently the CDOM spectral slope between 320 and 412 nm ($S_{320–412}$, nm^{-1}) are used as tracers for in situ production of autochthonous DOM (Table 1).

However, while these optical properties are clearly useful, especially as qualitative markers for identifying the presence and biogeochemical cycling of tDOC, it is still often unclear how accurate they really are as tracers of tDOC concentration across coastal gradients where tDOC undergoes extensive remineralization. Several studies have shown that some of the optical properties (a_λ, $S_{275–295}$) are related to tDOC composition in estuarine and coastal environments, and that these optical properties can therefore be used to quantify tDOC concentration (Fichot & Benner, 2012; Fichot et al., 2016; Hernes & Benner, 2003; Mann et al., 2016). However, on the one hand, terrigenous CDOM and FDOM may be more labile and lost preferentially relative to bulk tDOC, especially when subject to photodegradation (Benner & Kaiser, 2011; Moran et al., 2000; Osburn et al., 2009). Yet on the other hand, tDOC itself can only be estimated from proxy measures, and comparisons between optical properties and tDOC have primarily relied on lignin phenols as a biomarker to quantify tDOC. While lignin phenols unambiguously show that tDOC is present, they are only a small fraction of the bulk tDOC (Fichot & Benner, 2012; Louchouarn et al., 2000; Osburn & Stedmon, 2011), and may also decompose more easily than bulk tDOC during remineralization, especially from photodegradation (Benner & Kaiser, 2011; Cao et al., 2018; Hernes & Benner, 2003). This is further demonstrated by the fact that lignin phenols are scarce in the open-ocean DOC pool (Hedges et al., 1997; Meyers-Schulte & Hedges, 1986; Opsahl & Benner, 1997), although molecular and carbon isotope data suggest that oceanic DOC may in fact contain more tDOC than previously recognized (Cao et al., 2018; Medeiros et al., 2016; Zigah et al., 2017). Moreover, few studies have compared the various different optical properties comprehensively to evaluate which are the most reliable for tracing tDOC in natural samples with mixed sources. Where systematic comparisons have been conducted, they have been largely based on laboratory studies using DOM from a limited range of plant, soil, or microbial sources, and subject to purely photochemical or purely microbial degradation experiments (Hansen et al., 2016; M.-H. Lee et al., 2018). Specifically, Hansen et al. (2016) showed that individual optical properties depended on both source and DOM degradation processes, with photochemical and microbial degradation often causing opposing changes. They recommended that multiple optical properties should be used to evaluate DOM sources in a qualitative perspective but did not show any quantitative information. Similarly, M.-H. Lee et al. (2018) concluded that SUVA, BIX and FI are reliable to infer specific biogeochemical processes because they are rarely affected by UV irradiation, biodegradation and adsorption, respectively, but no statistical relationships were derived between optical properties and tDOC either. While these laboratory experiments have provided important insights, we do not know how closely these results reflect what happens in the coastal environment, where the DOM pool may consist of many more different sources, and physical, photochemical, and microbial processes interact in potentially complex ways (Antony et al., 2018; Bushaw-Newton & Moran, 1999; Grunert et al., 2021; Miller & Moran, 1997). Consequently, more environmental data sets are needed in which optical parameters can be directly compared and related to the actual tDOC concentration across a known gradient of tDOC remineralization.

Isotope analysis can provide clear identification of DOC sources in coastal waters. Because of biological isotope fractionation, tDOC produced by C3 plants is depleted in ^{13}C, leading to a more negative stable isotope ratio ($\delta^{13}C$) than DOC from primary production in aquatic environments (Boutton, 1991). Based on the known ranges of $\delta^{13}C$ from different sources (Fry & Sherr, 1989; Lamb et al., 2006), $\delta^{13}C$ is thus used to distinguish the presence and transformation of tDOC in coastal waters (Alkhatib et al., 2007; Han et al., 2021; S. A. Lee et al., 2020; Ye et al., 2018). Specifically, $\delta^{13}C_{DOC}$ values are used to quantify tDOC based on endmember mixing

Journal of Geophysical Research: Biogeosciences

10.1029/2024JG008147

Table 1
Description of Widely Used Optical Properties Indicating Sources and Compositions of DOM

Optical property	Provided information	Reference
a_λ (m^{-1})	Represents CDOM concentration, often linearly correlated to DOC and lignin phenol concentrations in different aquatic environments	Fichot and Benner (2011), Hernes and Benner (2003), Osburn et al. (2016), and Vantrepotte et al. (2015)
$S_{275–295}$ (nm^{-1})	Negatively correlated to DOM apparent molecular weight, exhibits exponential relationship with concentration of lignin phenols	Del Vecchio and Blough (2002), Fichot and Benner (2012), and Helms et al. (2008)
S_R	Higher values indicate higher content of low apparent molecular weight components in DOM; increases upon photo exposure	Helms et al. (2008)
$S_{320–412}$ (nm^{-1})	An indicator of freshly produced autochthonous marine DOM, strong linear correlation to DOC-specific a_λ during phytoplankton bloom	Danhiez et al. (2017)
$SUVA_{254}$ (L mg-C^{-1} m^{-1})	Shows linear relationship with aromaticity of DOM	Cartisano et al. (2018), Chin et al. (1994), Hur et al. (2006), and Weishaar et al. (2003)
FI	DOM is likely to be terrestrial when FI < 1.4, while is more marine-sourced with higher FI	Cory et al. (2010) and McKnight et al. (2001)
HIX	An indicator of content of humic substances or extent of humification in DOM, higher values corresponds to higher humification level	Ohno (2002)
BIX	An indicator of autochthonous biological activity, high values (>1) indicate dominance of aquatic DOM	Huguet et al. (2009)

models (Humborg et al., 2017; Ye et al., 2018; Zhou et al., 2021). Similarly, the deviations of DIC concentration and $\delta^{13}C_{DIC}$ values from their corresponding conservative mixing are used to calculate the remineralization of tDOC, because tDOC remineralization causes DIC production while lowers the $\delta^{13}C_{DIC}$ (Humborg et al., 2017; Samanta et al., 2015; Su et al., 2017). Thus, carbon stable isotope mass balances can provide quantitative estimates of tDOC concentration in samples with DOC from mixed sources, and of the prior remineralization of tDOC.

In this study, we used a multi-year time series of DOC concentration, DOC and DIC carbon stable isotope composition, and DOM optical analysis from coastal Southeast Asia. Southeast Asia's extensive tropical peatlands deliver around 10% of global land–ocean DOC flux (Baum et al., 2007; Huang et al., 2017; Moore et al., 2011), while the region's archipelagic geography and monsoon-driven ocean current reversal result in long water residence times on the shelf (Mayer et al., 2022), allowing the majority of tDOC to be remineralized within the shelf sea (Wit et al., 2018; Zhou et al., 2021). We used a carbon stable isotope mass balance approach to calculate both the percentage contribution of tDOC to the bulk DOC pool (tDOC%) and the proportion of tDOC that had been remineralized to DIC. This allows us to test how accurately different optical properties can quantify tDOC%, and also to test whether any of the optical properties change purely as a function of the extent of tDOC remineralization. In addition, we compared our environmental data to results obtained from laboratory tDOC remineralization experiments to examine whether the changes in optical properties during such simplified experiments reflect the patterns we observed in our environmental data. This study not only provides a large biogeochemical and optical data set from a hotspot for carbon cycling, but also demonstrates the validity of applying spectroscopic techniques to broadly trace tDOC quantitatively in natural environments.

2. Data Set and Methods

2.1. Data Sets Used in the Present Analysis

The main data set used in the present analysis is a multi-year time series of DOC concentration, stable carbon isotope composition, and optical properties collected in the Singapore Strait. In the Singapore Strait, the monsoon system causes a seasonal reversal of water currents (Mayer et al., 2022; Susanto et al., 2016; van Maren & Gerritsen, 2012): this causes tDOC originating from peatlands on Sumatra to be transported to our study site during the Southwest (SW) Monsoon (May to September), while water from the South China Sea with a mostly marine DOC pool is delivered during the Northeast (NE) Monsoon (November to March; Figure S1 in Supporting Information S1; Zhou et al., 2021).

Because we lack optical data from the peatland-draining rivers on Sumatra that form the riverine endmember for our study site (Martin et al., 2022; Zhou et al., 2021), we complement our analysis using two other data sources. For CDOM absorption (as a_{440}), we calculated the discharge-weighted average for the main peatland-draining rivers based on Siegel et al. (2019) and Wit et al. (2018), detailed in Section 2.5.2. The resulting values of a_{440} and DOC follow the same CDOM-DOC relationship found for the various peatland-draining rivers in Sarawak (Figure S2 in Supporting Information S1; Martin et al., 2018). This indicates that the tDOC composition and optical properties are broadly similar across Southeast Asian peatlands, which is also consistent with the fact that DOC concentrations in peatland-draining rivers follow a single, strong relationship to catchment peatland cover across both Sumatra and Borneo (Rixen et al., 2022). Therefore, for the other optical properties, we used CDOM and FDOM data acquired from three expeditions in rivers in Sarawak, Borneo (Martin et al., 2018; Zhou et al., 2019). The Sarawak data were divided into three categories: peat-majority rivers (salinity < 1) with catchment peatland coverage $\geq$50%, non-peat-majority rivers (salinity < 1) with catchment peatland coverage <50%, and Sarawak estuarine and coastal water (salinity ≥ 1).

2.2. Singapore Strait Timeseries Sampling

The Singapore Strait timeseries data were collected from October 2017 to July 2021. Water samples were collected from 5-m depth at two sites in the Singapore Strait using a Niskin bottle. Sampling was undertaken monthly except during pandemic-related restrictions (March to June 2020). The water was filtered onboard through a pre-rinsed 0.22 μm polyethersulfone membrane (Supor, Merck Millipore) with a peristaltic pump for analyses of DOC and DIC concentrations, CDOM and FDOM spectra, stable isotope composition of DOC and DIC ($\delta^{13}C_{DOC}$ and $\delta^{13}C_{DIC}$) and total alkalinity (TA). All vials and tubes had been washed with 1 M HCl and ultrapure water (18.2 MΩ cm^{-1}). Amber borosilicate vials for DOC and optical measurements were pre-

combusted at 450°C for 4 hr after washing. Specifically, CDOM and FDOM spectra were measured upon carried back to our lab while samples of DIC and TA were stored dark at +4°C and analyzed 1 day after collection. Samples of DOC (30 mL) were acidified with 100 µL 50% sulfuric acid to achieve pH ≤ 2 and stored dark at +4°C before analysis. Samples of $\delta^{13}C_{DOC}$ were stored dark and frozen, and thawed and acidified before sent out for analysis, while samples of $\delta^{13}C_{DIC}$ were kept dark at room temperature (22 ± 0.5°C). Detailed information about collection and preservation of biogeochemical samples were provided in a previous publication (Zhou et al., 2021). At each station, a depth profile of salinity and temperature was measured using a fastCTD Profiler (Valeport Ltd). The water column typically does not show stratification (Martin et al., 2022).

2.3. Sample Analysis

2.3.1. Dissolved Carbon and Total Alkalinity Analysis

Triplicate DOC samples (30 mL) were analyzed at room temperature (22 ± 0.5°C) on a Shimadzu TOC-L system with a high-salt combustion kit. For each sample, 5–7 replicate injections were performed to ensure that the coefficient of variation was less than 2%. For each run, potassium hydrogen phthalate standards were used for calibration, and deep-sea water (42–45 µmol/L DOC) from the University of Miami, USA was analyzed as certified reference materials (long-term mean and standard deviation from our 2017–2022 analysis: 46.7 ± 4.2 µmol/L). DIC was analyzed on an Apollo SciTech AS-C5 DIC analyzer at room temperature (22 ± 0.5°C). Each sample was measured 3–5 times to obtain a relative standard deviation less than 0.1%. Certified reference material from Scripps Institution of Oceanography (Batch 172) or an in-house secondary standard of Singapore Strait seawater was used for calibration. The analytical precision was ±0.15%.

TA was analyzed at room temperature (22 ± 0.5°C) on an Apollo SciTech AS-ALK2 titrator with a ROSS combination glass pH electrode (Orion 8302BNUMD), conducting the Gran titration (Gran, 1952) automatically. The titration was conducted with a 25-mL aliquot and 0.1 M hydrochloric acid (HCl) and repeated 2–4 times for each sample. The CRM or secondary standard above was used for calibration and the analytical precision was ±0.13%.

Stable isotope ratio of DOC ($\delta^{13}C_{DOC}$) samples were stored at −20°C, then thawed and acidified with 35 µL concentrated HCl to pH of 2–3 and analyzed at the Ján Veizer Stable Isotope Laboratory, University of Ottawa, Canada (2-sigma analytical precision of ±0.4%).

Stable carbon isotope ratio of DIC ($\delta^{13}C_{DIC}$) samples were stored dark at room temperature (22 ± 0.5°C) until analysis. Samples were analyzed using a Gas Bench connected to an isotope ratio mass spectrometer, partly at the Stable Isotope Facility, University of California, Davis (analytical precision of ±0.1‰), and partly in the Marine Geochemistry Laboratory, Nanyang Technological University, Singapore (analytical precision of ±0.2‰). Details of the measurements in Singapore were described in Zhou et al. (2021). Interlaboratory correction was performed for the measurements in Singapore using the international consensus value of $\delta^{13}C_{DIC}$ of the Dickson CRM (0.78‰; Cheng et al., 2019), and this correction mostly accounted for less than 0.4‰.

2.3.2. Optical Analysis

Samples for CDOM and FDOM were analyzed at room temperature (22 ± 0.5°C) on the day of collection or after overnight storage at 4°C. CDOM absorption was measured on a Thermo Evolution 300 dual-beam spectrophotometer from 230 to 900 nm at 1-nm resolution in 10-cm or 2-mm quartz cuvettes with ultrapure water as a reference. They were baseline-corrected according to Green and Blough (1994) and further analyzed using the R package "hyperSpec" (Beleites & Sergo, 2018). We calculated the following properties: a_{350} or a_{440} (m^{-1}), $S_{275–295}$ (nm^{-1}; Helms et al., 2008), $S_{320–412}$ (nm^{-1}; Danhiez et al., 2017), S_R (Helms et al., 2008) and $SUVA_{254}$ (L mg-C^{-1} m^{-1}; Weishaar et al., 2003).

FDOM steady-state fluorescence excitation–emission matrices (EEMs) were measured on a HORIBA Jobin Yvon FluoroMax-4 fluorometer in a 1-cm or 3-mm quartz cuvette at excitation wavelength of 250–450 nm with 5-nm intervals and emission wavelength of 290–550 nm with 2-nm intervals, with 5 nm for both bandwidths. EEMs of ultrapure water were analyzed to record Raman and Rayleigh scattering. EEMs were processed using the Matlab drEEM toolbox (Murphy et al., 2013) to achieve inner filter effects correction, blank subtraction, and conversion to Raman units (RU; Lawaetz & Stedmon, 2009). We calculated the fluorescence index (FI; Cory et al., 2010), humification index (HIX; Ohno, 2002) and biological freshness index (BIX; Huguet et al., 2009).

The calculations of these optical properties and the information that they are considered to provide are described in Table 1.

2.4. Photodegradation Experiments

We used data from the same photodegradation experiments reported by Zhou et al. (2021) that were conducted with water samples from a peatland-draining river on Borneo (Maludam River) and from the Singapore Strait during the SW Monsoon. Although we used the same data set as the previous publication, our purpose here is to identify whether any of the properties is quantitatively related to the extent of tDOC photochemical remineralization, which was not addressed in Zhou et al. (2021). The experimental methods are described in detail in Zhou et al. (2021); briefly, 30 mL filtered water was added into replicate cylindrical quartz cells (50 mm pathlength, 50 mm diameter) with Teflon screw caps, and irradiated under a xenon lamp with daylight optical filter in an Atlas Suntest CPS + solar simulator. Dark controls of filtered water were placed in Duran bottles fully wrapped with aluminum foil in the solar simulator. Two replicate cells of samples under light exposure and two replicates of the control samples were taken at each time point for DOC concentration and optical measurements.

2.5. Statistical Analysis

2.5.1. Parallel Factor Analysis

PARAFAC can partition fluorescence EEMs into underlying fluorescent components to characterize and quantify the relative contribution of different fractions (Cory & McKnight, 2005; Murphy et al., 2013; Stedmon & Bro, 2008). A total of 550 sample EEMs, including environmental data from the Singapore Strait and Sarawak, Borneo, and experimental data from photodegradation and bio-incubation for coastal seawater and Maludam water (Zhou et al., 2019, 2021), were analyzed by PARAFAC using the drEEM toolbox in MATLAB (Murphy et al., 2013). Eleven EEMs were excluded because they were identified as outliers by visual inspection. A five-component model was generated and validated by split-half analysis. The excitation and emission peak wavelengths of the 5 components (C1–C5, Figure S3 in Supporting Information S1) were compared with other studies and with the OpenFluor database (Coble, 1996; Murphy et al., 2008, 2014; Osburn et al., 2016; Stedmon & Markager, 2005a; Stedmon et al., 2003; Zhou et al., 2019) to attribute possible sources of the DOM fractions that they represent (Table S1 in Supporting Information S1). The fluorescence intensity at the excitation and emission maximum (Fmax) is a measure of the contribution to total fluorescence and of the concentration of each DOM fraction represented by the corresponding PARAFAC component.

2.5.2. Mixing Models and Carbon Isotope Mass Balance Calculation

We assessed the mixing behavior of the optical parameters across the whole salinity gradient. Moreover, we used a carbon isotope mass balance approach to calculate the amount of tDOC that had been remineralized, following the approach of previous publications (Humborg et al., 2017; Samanta et al., 2015; Su et al., 2017; Zhou et al., 2021). Specifically, we used two-endmember mixing models to estimate expected distributions of measured parameters across the salinity gradient for purely conservative mixing between a riverine and a marine endmember. We obtained riverine endmember values of $\delta^{13}C_{DOC}$, $\delta^{13}C_{DIC}$, DIC and TA (Table S2 in Supporting Information S1) by taking discharge-weighted averages of data from the four main peat-draining rivers on Sumatra (the Indragiri, Kampar, Siak and Batanghari in Figure S1b in Supporting Information S1) that are the most plausible sources of peatland tDOC to the Singapore Strait (Siegel et al., 2009, 2019; Wit et al., 2018; Zhou et al., 2021). The resulting riverine endmember value for a_{440} was corroborated by the fact that the a_{440} and DOC fall onto the same CDOM–DOC relationship found for the various peatland-draining rivers in Sarawak (Figure S2 in Supporting Information S1; Martin et al., 2018). This suggests that peatland tDOM pools and their optical properties are quite similar across Southeast Asian peatlands, and that variation in tDOC concentration among rivers is primarily a function of catchment peatland coverage rather than reflecting differences in tDOM characteristics (Rixen et al., 2022). Since $\delta^{13}C_{DOC}$ in peatland-draining rivers of Southeast Asia mostly ranges between −30‰ and −28‰ (Evans et al., 2014; Gandois et al., 2014; Zhu et al., 2020), we adopted an approximated value of −29‰ as the riverine endmember. Photodegradation and combined photo-biodegradation of tDOC can cause fractionation of −1.4‰ to −5.8‰ between the original $\delta^{13}C_{DOC}$ and the produced $\delta^{13}C_{DIC}$ values (Opsahl & Zepp, 2001; Osburn et al., 2001; Spencer, Stubbins, et al., 2009). Given that peatland-derived tDOC in Southeast Asia appears to be fairly refractory to direct biodegradation but shows high photo-lability (Nichols &

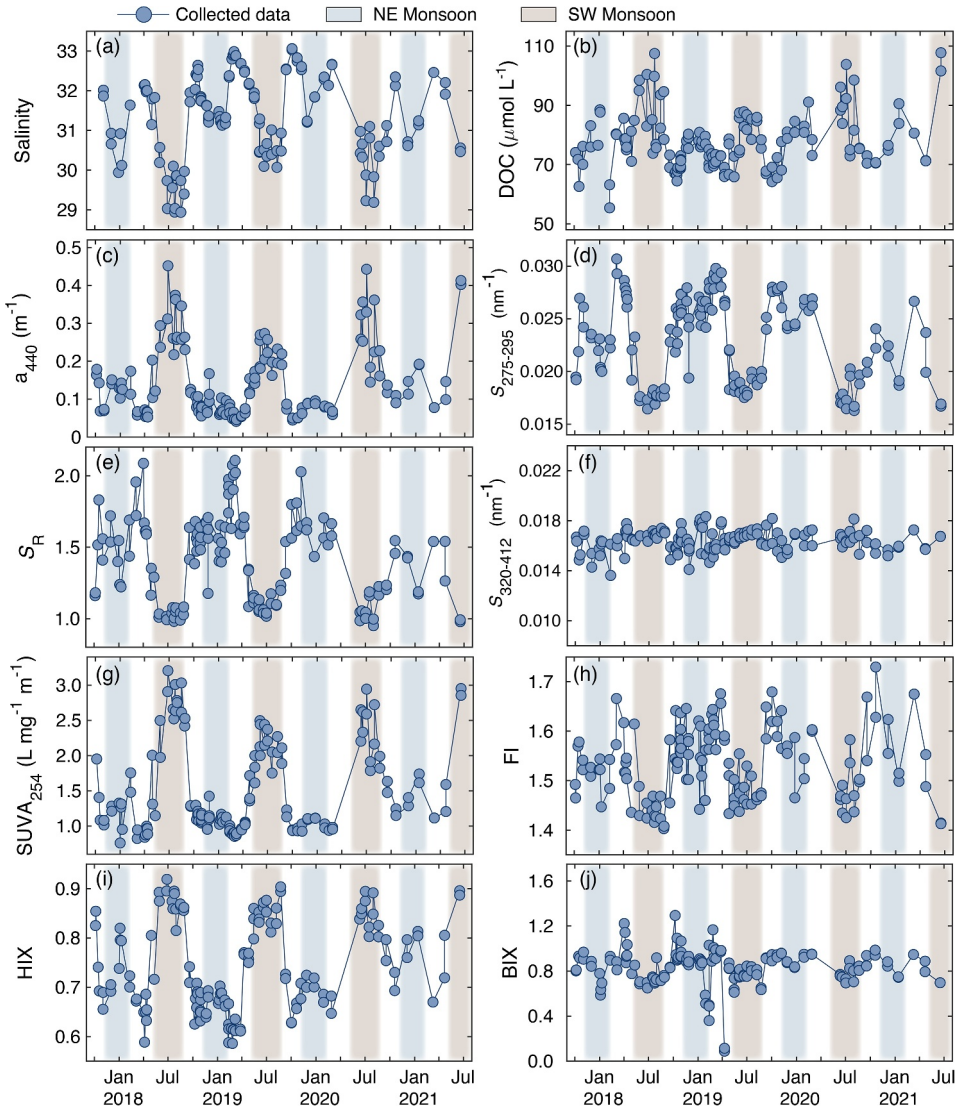

Figure 1. Timeseries data of salinity, Dissolved organic carbon (DOC) concentration and optical properties in the Singapore Strait. Data from Northeast (NE) Monsoon and Southwest (SW) Monsoon are distinguished by different shading colors. Detailed information about optical properties (a_{440}, $S_{275–295}$, S_R, $S_{320–412}$, $SUVA_{254}$, fluorescence index [FI], humification index [HIX] and biological index [BIX]) are listed in Table 1. Salinity, DOC concentration, a_{440}, $S_{275–295}$, S_R, $SUVA_{254}$, FI and HIX presented seasonal changes driven by the monsoonal current reversal, while $S_{320–412}$ and BIX showed limited or no seasonality.

Martin, 2021; Zhou et al., 2021), we adopted a fractionation of −3‰, thus taking −32‰ as the $\delta^{13}C_{DIC}$ value for remineralized tDOC in our calculation. Marine endmember values were determined as averages of the measurements during late February and March, when marine water from the open South China Sea, which contains little tDOC, predominates in the Singapore Strait (Figure 1). All riverine and marine endmember values are provided in Table S2 in Supporting Information S1. The fractional contributions of freshwater and seawater were determined from salinity.

To quantify the remaining tDOC concentration and how much tDOC had already been remineralized to DIC, we assumed that tDOC is the only source of remineralized terrigenous carbon while terrigenous particulate organic carbon (POC) does not contribute, and that autochthonous DOC cycling does not influence our estimation. These assumptions are discussed in Section 4.1. The equations for the carbon isotope mass balance calculation are provided in Supporting Information S1 (Samanta et al., 2015; Zhou et al., 2021). Briefly, the concentration of tDOC in each sample was calculated from the measured $\delta^{13}C_{DOC}$ and DOC concentration using a two-

endmember isotope mixing model based on the riverine and marine endmember $\delta^{13}C_{DOC}$ values. We refer to this as "remaining tDOC concentration" because it represents the fraction of the initial tDOC input that remains in form of DOC, as opposed to the fraction that has been remineralized. We divided the remaining tDOC concentration by the measured DOC concentration of our collected samples to obtain the percentage contribution of tDOC in the bulk DOC (tDOC%). We then used the observed deviation of the $\delta^{13}C_{DIC}$ from conservative mixing (Figure S4 in Supporting Information S1) to back-calculate how much tDOC had already been remineralized for each sample prior to that sample water reaching our sampling site, following the approach used in previous studies (Humborg et al., 2017; Samanta et al., 2015; Su et al., 2017; Zhou et al., 2021). This calculation is based on the deviation of $\delta^{13}C_{DIC}$ from the predicted conservative mixing, together with the known stoichiometric effects of primary production, remineralization, calcium carbonate production and dissolution, and air-sea CO_2 exchange on the deviations of DIC and TA from their conservative mixing values (Figure S4 in Supporting Information S1; Zeebe & Wolf-Gladrow, 2001), and on the fractionation of $\delta^{13}C_{DIC}$ during these processes (Opsahl & Zepp, 2001; Osburn et al., 2001; Spencer, Aiken, et al., 2009). We refer to the sum of remaining tDOC and remineralized tDOC as the "total initial tDOC concentration." The extent of tDOC remineralization was then calculated as the ratio of remineralized tDOC to the total initial tDOC.

The mixing patterns of both the remaining tDOC and total initial tDOC showed a linear (and therefore conservative) relationship to salinity (see Section 3.3). We therefore used these relationships to estimate the apparent and actual riverine endmember tDOC concentrations by extrapolating both relationships back to salinity 0. The errors of tDOC extrapolation were the standard deviations calculated from Monte Carlo simulation by taking all uncertainties of measurements and calculation into consideration (Table S2 in Supporting Information S1) and recalculating 10,000 times. Similarly, the apparent riverine endmember value of a_{440} was obtained by extrapolating our a_{440} timeseries data to salinity 0 based on the conservative mixing model. The actual riverine endmember a_{440} was obtained from the discharge-weighted average as explained in the previous paragraph. The errors of apparent and actual riverine endmember a_{440} were obtained directly from the linear regression of a_{440} against salinity and as the standard deviation from the discharge-weighted average calculation, respectively. These endmember values are presented in Table S3 in Supporting Information S1.

3. Results

3.1. Temporal Variation of DOM Optical Properties in the Singapore Strait

There is a seasonal change in biogeochemistry in the Singapore Strait driven by the monsoonal current reversal. The extended timeseries data in the present study demonstrates similar seasonal patterns compared to previous publications (Martin et al., 2021, 2022; Zhou et al., 2021). Here, we further examine additional optical parameters ($S_{320–412}$, FI, BIX, HIX, and C2 from PARAFAC analysis) to assess the application of spectroscopic techniques to quantify the concentration and remineralization of tDOC in the natural environment directly, instead of using other proxies such as lignin phenols to represent the bulk tDOC.

During the SW Monsoon (May to September), currents carry freshwater from the east coast of Sumatra to our study site in the Singapore Strait, causing salinity to drop from approximately 33 to around 29 (Figure 1a and Figure S1a in Supporting Information S1). DOC and CDOM (a_{440}) concentrations increased by, respectively, 1–2 and 2–10 times compared to other seasons, with maximum concentrations showing clear interannual variability (Figures 1b and 1c). $S_{275–295}$ and S_R showed the lowest values during the SW Monsoon, in the range of 0.016–0.020 nm^{-1} and 0.95–1.23, respectively (Figures 1d and 1e). In contrast, $SUVA_{254}$ and HIX reached peak values of higher than 3.3 L $mg\text{-}C^{-1}$ m^{-1} and 0.9, respectively (Figures 1f and 1g). This seasonality in the optical properties indicates a large amount of tDOC input by freshwater. During the NE Monsoon and the following early inter-monsoon season (December to March), water without much terrestrial input flows from the South China Sea to the study site, resulting in relatively high $S_{275–295}$, low S_R, low $SUVA_{254}$ and low HIX. In contrast, FI and BIX tended to have consistently low values during the SW Monsoon, respectively at around 1.4 and 0.7, but exhibited variable values in the other seasons, so that the overall seasonal contrast was less strong than that for optical properties typically associated with tDOC (Figures 1h and 1i). Finally, $S_{320–412}$ showed very little variation and no seasonality, with values mostly from 0.015 to 0.019 nm^{-1} (Figure 1j).

3.2. Temporal Variation of PARAFAC Components in the Singapore Strait

Five fluorescent components (C1–C5) were identified by PARAFAC analysis (Figure S3 and Table S1 in Supporting Information S1), explaining 99.4% of the variability of the data set. Among these 5 components, C1, C2, and C3 emitted mostly at visible wavelengths, which may suggest a large contribution of molecular conjugation or interaction (Y. Chen et al., 2020; Coble, 1996; Del Vecchio & Blough, 2004a). Specifically, C1 has been identified in different water bodies (Stedmon & Markager, 2005a) and is typically associated with fulvic acid fluorophores. Emission peaks of C2 at around 430 nm with two excitation maxima at 250 and 430 nm have been respectively assigned as humic-like components peak A and C in previous work (Coble, 1996), and have been widely thought to represent DOM fractions with high apparent molecular weight (Jaffé et al., 2014; McKnight et al., 2001; Stedmon et al., 2003; Yamashita et al., 2008). C2 has been reported to be highly correlated with lignin phenol concentrations (Yamashita et al., 2015) and is found only at low intensities in the open ocean (Murphy et al., 2008), thus is considered to be terrestrially derived. Additionally, DOC-normalized C2 intensity was used previously to estimate tDOC percent contribution in the Sarawak FDOM data set (Zhou et al., 2019). C3 also resembles the maxima characteristic of peak A but possessed a wider emission wavelength range, which has been found dominated by DOM derived from forest and wetland regions (Stedmon et al., 2003). Although C4 was considered related to marine humic-like material in some studies (Coble, 1996; Yamashita et al., 2015), it was related to microbial processed materials (Grunert et al., 2021; Osburn et al., 2016) and was found to have significant terrestrial signals in Southeast Asia (Harun et al., 2016; Zhou et al., 2019) and in the boreal region (Kothawala et al., 2012). In the present study, the terrestrial origin of C4 was proven by the consistent seasonal change with freshwater input caused by monsoon-driven currents. Finally, C5 shows high similarity to peak T and peak B, which have been considered as protein-like fluorophores produced from microbial processes, and usually associated with fresh phytoplankton-produced DOM (Coble, 1996; Kowalczuk et al., 2013; Stedmon & Markager, 2005b; Yamashita & Tanoue, 2003; Yang & Hur, 2014). These components attributions were validated by comparison to the OpenFluor database, in which humic-like components include C1–C4 in the present study and protein-like components include C5 (Murphy et al., 2014).

Generally, the signals of C1–C4 exhibited similar seasonal changes during the 4 years, with high fluorescence contribution during the SW Monsoon, roughly 4–11 times greater than those during other seasons (Figures 2a–2d). This seasonality is consistent with the reported attribution of PARAFAC components mentioned above and the monsoon-driven freshwater delivery to the sampling site. There was also an interannual variability of peak values, consistent with that observed in DOC concentration, a_{440} and $SUVA_{254}$. Among these four components, their intensities followed an order of C3 > C2 > C4 > C1. In contrast, Fmax of C5 stayed within the range of 0.015–0.035 RU without obvious seasonality (Figure 2e). This suggests that there is a steadily low level of marine-sourced DOM in the Singapore Strait that is hardly influenced by seasonal water advection and mixing.

3.3. Carbon Isotope Mass Balance and Preferential CDOM Loss Relative to tDOC

During the SW Monsoon, $\delta^{13}C$ tended to be more negative for both the DOC and DIC pool, with values mostly from −25.5‰ to −24‰ and −1.8‰ to −0.9‰, respectively (Figures 3a and 3b), indicating the large contribution of terrigenous carbon. Based on our carbon isotope mass balance, the remaining tDOC and total initial tDOC concentrations reached peak values of 50–60 and ∼120 μmol L^{-1}, respectively, during the SW monsoon (Figures 3c and 3d). During the NE Monsoon and the following inter-monsoon seasons, in contrast, the timeseries data exhibited the most enriched $\delta^{13}C_{DIC}$ and $\delta^{13}C_{DOC}$ and thus the lowest values for the remaining tDOC and total initial tDOC concentrations.

We observed linear relationships with salinity (and therefore apparent conservative mixing) for both the remaining ($r^2 = 0.57$, $p < 0.01$) and the total initial tDOC ($r^2 = 0.45$, $p < 0.01$) concentrations (Figure 3e). By extrapolating these relationships back to salinity 0, we inferred an apparent riverine tDOC concentration of 386 ± 97 μmol L^{-1} and an actual riverine tDOC concentration of 814 ± 133 μmol L^{-1}. Our actual riverine tDOC concentration is within the uncertainty range of the discharge-weighted average DOC (890 ± 159 μmol L^{-1}) reported from the four main peat-draining rivers in Sumatra that represent the most plausible source of tDOC input to Singapore (Wit et al., 2018). Our estimate is also very close (within 9%) to the value published previously based on a shorter timeseries (Zhou et al., 2021). The difference between the apparent and actual endmember tDOC concentrations indicates that, on average, 53% of the initial tDOC is remineralized before reaching our

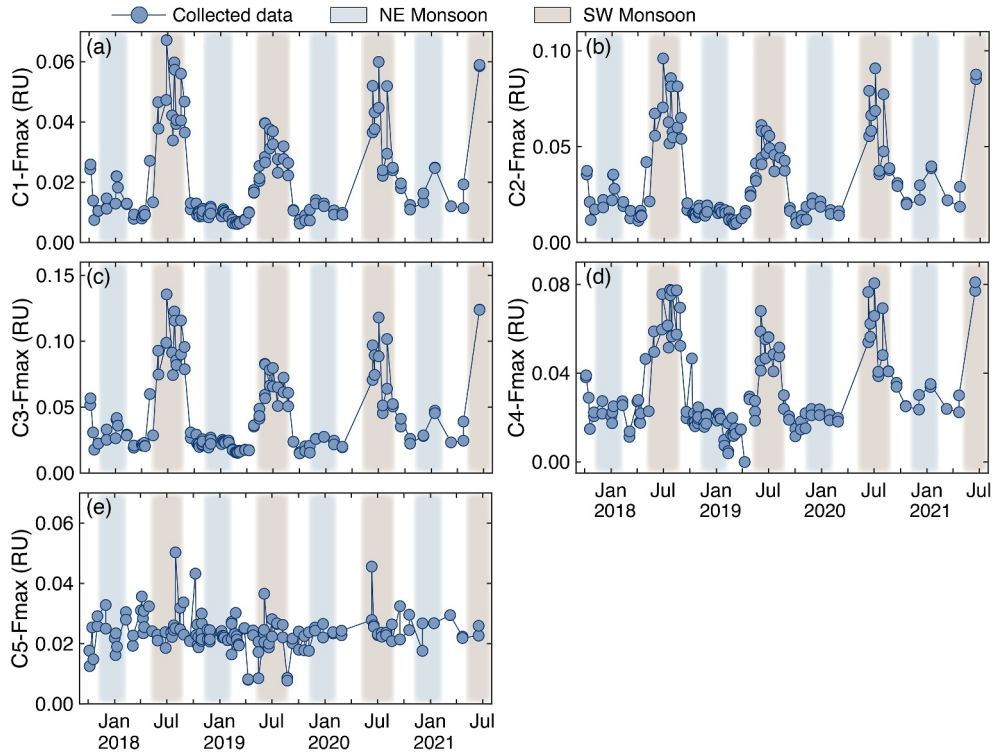

Figure 2. Timeseries data of fluorescent dissolved organic matter (FDOM) component intensities derived from parallel factor analysis analysis. Components 1–4 (C1–C4) were identified as terrestrial components as their variability was consistent with seasonal freshwater input. The highest values were observed during the Southwest (SW) Monsoon when terrestrial dissolved organic matter (tDOM) is delivered from the west coast of Sumatra by water currents while consistent low values were observed during the Northeast (NE) Monsoon. Component 5 (C5), which was attributed to marine-sourced DOM, showed little variability.

sampling site. The remaining tDOC concentration measured at our site is therefore the result of both remineralization and physical dilution with open seawater from the South China Sea.

We quantified CDOM using the a_{440} rather than a_{350} to allow a direct comparison to the data published from Sumatra (Siegel et al., 2009, 2019). CDOM a_{440} showed a strong linear relationship with salinity in the Singapore Strait ($r^2 = 0.76$, $p < 0.01$, Figure 3f), from which we inferred an apparent riverine endmember a_{440} of $2.7 \pm 0.2\ m^{-1}$. This is 77% lower than the discharge-weighted riverine endmember a_{440} of $10.3 \pm 0.8\ m^{-1}$ that we calculated based on the data in Siegel et al. (2019) and Wit et al. (2018). We therefore conclude that on average $74 \pm 9\%$ of CDOM absorption is lost before reaching our sampling site. This shows that there is preferential loss of CDOM relative to tDOC.

3.4. Mixing Patterns of DOM Optical Properties in Singapore and Sarawak

The compiled Singapore and Sarawak carbon and optical data plotted against salinity showed that the DOM properties at the two sites broadly fell within an overlapping range on the same mixing continuum (Figure 4). The Sarawak data showed a clear distinction for DOC concentration and for a_{440} of samples from rivers with >50% and <50% peatland in their catchments (squares in Figure 4). Clear differences between peat-majority and non-peat-majority rivers were also seen for $SUVA_{254}$, FI, HIX, and BIX, but less so for the CDOM spectral slope parameters. At low salinities (<25), corresponding to estuarine samples, high variability for DOC concentration, a_{440} and $SUVA_{254}$ was observed while the values for $S_{275-295}$, S_R, FI, HIX and BIX were less variable (triangles in Figure 4).

Between salinities of 27–33, corresponding to more mixed coastal waters beyond the dominant influence of a single river, the values of these DOM properties for Singapore and Sarawak coastal water largely overlapped for a given salinity (triangles and circles in Figure 4). Given that the marine endmember water for Singapore and

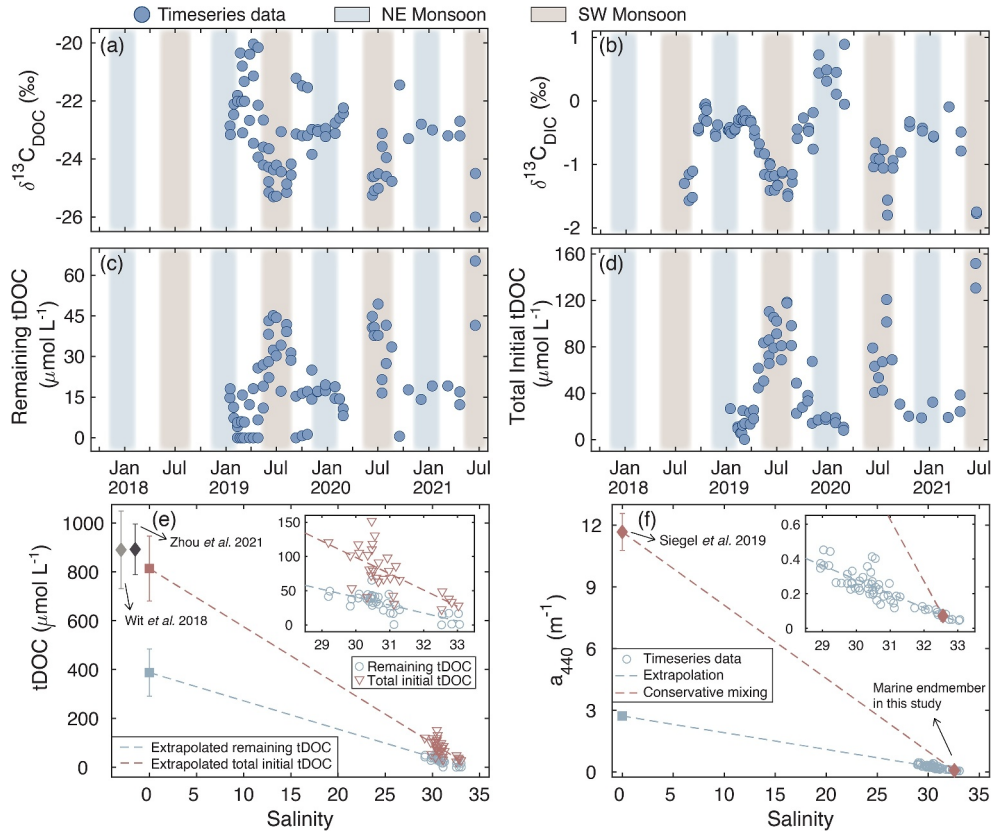

Figure 3. Timeseries data of stable carbon isotope ratios and terrestrial dissolved organic carbon (tDOC) concentrations, and mixing behaviors of tDOC and chromophoric dissolved organic matter (CDOM). (a) $\delta^{13}C_{DOC}$ and (b) $\delta^{13}C_{DIC}$ presented the most depleted values during the SW Monsoon due to freshwater input, while (c) the remaining tDOC and (d) total initial tDOC concentrations showed the highest values during this season. (e) The results of conservative mixing for tDOC concentrations suggested that on average 53% of tDOC is remineralized (error bars represent standard deviations), while (f) on average 74% of CDOM is bleached before reaching our study site, with error bars as the standard deviation from the discharge-weighted average calculation (red) and directly from the linear regression of a_{440} against salinity (blue).

Sarawak is the southern South China Sea, the overlap in DOM properties for a given salinity suggests that the riverine endmembers from Sarawak and Sumatra have similar average tDOM composition and optical properties, as also suggested by the similar relationship of CDOM a_{440} to DOC concentration for the river data (Figure S2 in Supporting Information S1). Because optical properties other than a_{440} had not been measured in rivers on Sumatra, we therefore used the freshwater data from the river systems in Sarawak to provide indicative ranges of these parameters for samples of pure tDOC in our further analysis of the Singapore data below.

3.5. Relationships of Optical Properties to tDOC Content

Our isotope mass balance calculation for the Singapore Strait timeseries allows us to estimate for each sample both the proportion of the bulk DOC pool that is tDOC and the amount of initially present tDOC that has been remineralized. We can therefore test how well the different optical properties are related to the tDOC content and whether they reflect the extent of prior remineralization. Given the similarity in DOM optical properties between our Singapore and Sarawak coastal water data (Figure 4 and Figure S2 in Supporting Information S1), we used the river data from Sarawak (at salinity 0) to provide an estimated range of values for the optical properties at 100% tDOC, prior to experiencing remineralization in the coastal environment.

Most of the optical properties showed significant relationships with the percentage of the remaining tDOC to the bulk DOC (tDOC%, Figure 5, statistical parameters are listed in Table 2). Consequently, a correlation matrix (Figure S5 in Supporting Information S1) shows that most of the optical properties are strongly correlated with

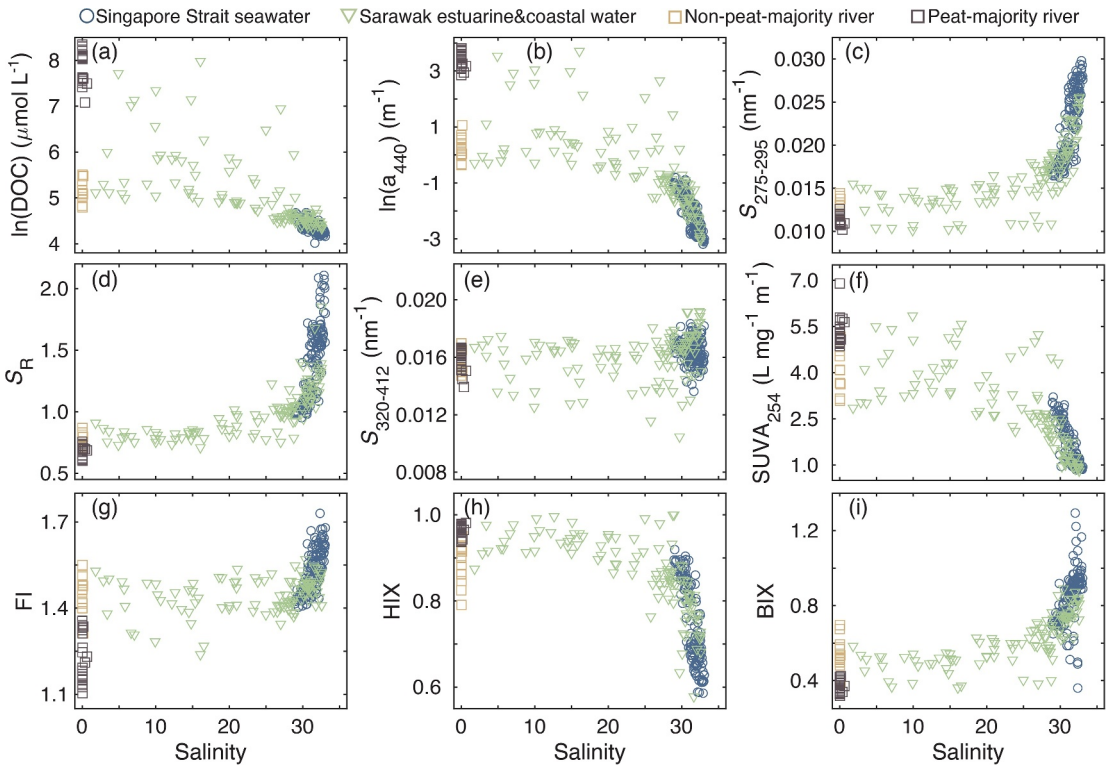

Figure 4. Dissolved organic carbon (DOC) concentration and optical properties (Table 1) of coastal water in the Singapore Strait, and of rivers and estuarine/coastal waters in Sarawak (Borneo) against salinity. River data from Sarawak are distinguished by whether the catchment has >50% (peat-majority river) or <50% (non-peat-majority river) peatland. For all parameters, the data from the Singapore Strait fall within the same mixing continuum as coastal waters from Sarawak.

each other and with tDOC% (mostly $r \geq 0.75$), except for somewhat weaker correlations with FI ($r = 0.67$–0.73) and weak or non-significant correlations (mostly $r < 0.4$) for BIX and $S_{320–412}$. Specifically, a_{440} presented a strong and linear relationship with tDOC% (Figure 5a), although owing to the preferential CDOM loss (Figures 3e and 3f), this relationship deviated from the river data. The spectral slope properties $S_{275–295}$ and S_R showed exponential relationships with tDOC%, with both r^2 of 0.55. When the relationships were extrapolated to 100% tDOC, they fell in the range of the Sarawak river data (Figures 5b and 5c), suggesting that these properties are applicable across the full range of tDOC%. The CDOM spectral slope $S_{320–412}$, which is indicative of fresh primary production of DOM (Danhiez et al., 2017), did not vary much throughout the whole tDOC% range (Figure 5d). $SUVA_{254}$ was linearly related to tDOC% and had the highest r^2 (0.66) of any of the optical properties (Figure 5e). Moreover, the relationship also fell within the range of the river data when extrapolated to 100% tDOC. Furthermore, compared to $S_{275–295}$ and S_R, $SUVA_{254}$ showed less scatter around the linear fitting line and possessed relatively narrower confidence and prediction intervals. For the fluorescence properties, there was a linear relationship between FI and tDOC% (Figure 5f) and the extrapolation fell within the range of collected river data, although the river values showed relatively large scatter. In contrast, HIX showed an exponential relationship with tDOC% and the relationship did not extrapolate into the range of the river data (Figure 5g). There was no relationship of BIX against tDOC% because BIX, like $S_{320–412}$, is more related to autochthonous marine DOM (Huguet et al., 2009). Finally, the DOC-normalized Fmax value of PARAFAC component 2 (C2-Fmax/DOC), which was previously used to estimate tDOC contribution in Sarawak estuaries (Zhou et al., 2019), was linearly related to tDOC%, showing similarly high r^2 (0.64) as $SUVA_{254}$ and falling in the range of the river data when extrapolated to salinity 0 (Figure 5i).

3.6. Relationships of Optical Properties to tDOC Remineralization

Our isotope mass balance showed that the tDOC had experienced a varying extent of remineralization (quantified as the percentage of remineralized tDOC to total initial tDOC) before reaching our sampling site. Unlike the strong relationships with tDOC%, none of the optical properties were related to the extent of tDOC

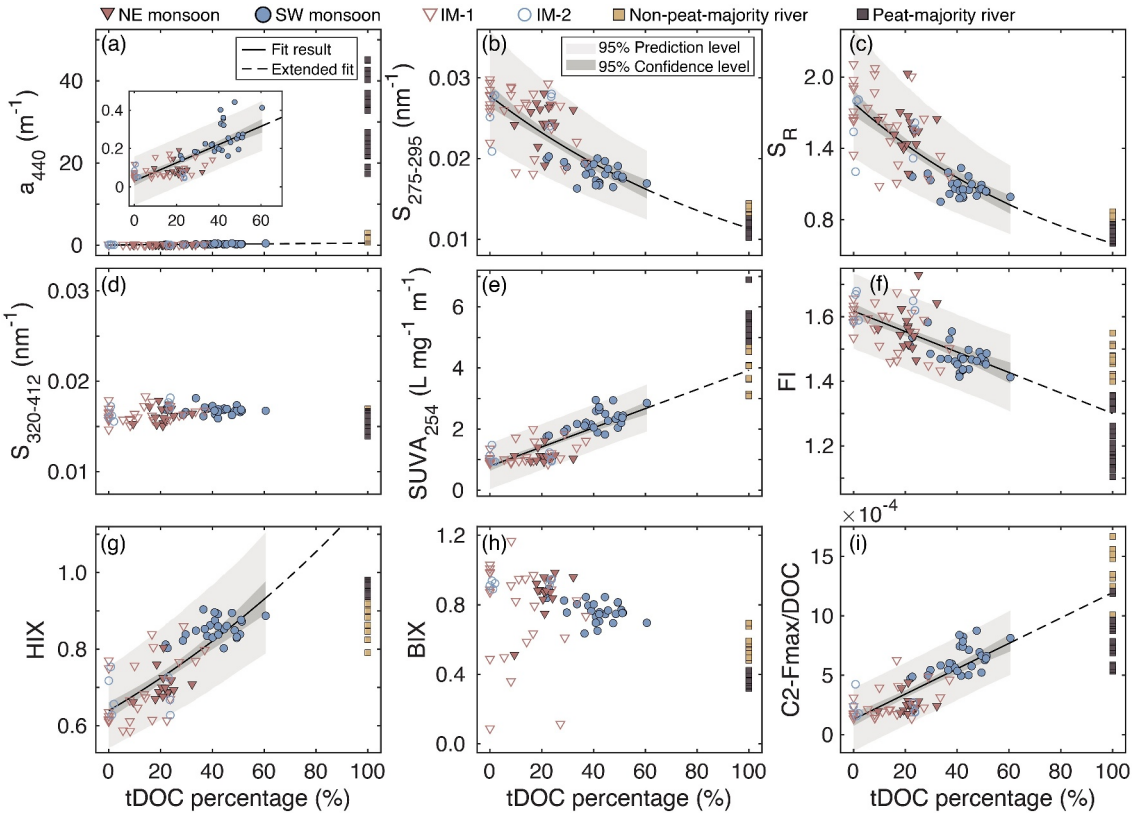

Figure 5. Relationships between optical properties (information listed in Table 1) and percentage contribution of terrestrial dissolved organic carbon (tDOC) to total DOC (tDOC%). The relationships were calculated only with the Singapore Strait data during NE Monsoon, Inter-Monsoon-1 (IM-1, the intermonsoon after NE Monsoon), SW Monsoon and Inter-Monsoon-2 (IM-2, the intermonsoon after SW Monsoon), but were extrapolated to 100% tDOC to compare to the reference river data from Sarawak. Shaded areas represent 95%prediction level (light gray) and 95% confidence level (dark gray).

remineralization, even though the extent of tDOC remineralization ranged from 7% to 75% during the SW Monsoon (Figure 6). This suggests that although most of the optical properties can be used as tracers of tDOC%, they do not appear to be sensitive to the extent of tDOC remineralization from complex biogeochemical processes in the natural environment. We restricted this analysis to include only data from the SW Monsoon as this is the only season with sufficiently large tDOC input to quantify the remineralization percentage accurately. The absolute concentration of tDOC is much lower in the other seasons, with both the remaining and total initial tDOC mostly less than 30 μmol L^{-1} (Figures 3c and 3d). Although small variations in $\delta^{13}C_{DIC}$ only give small values of

Table 2
Summary of Statistical Relationships of Optical Properties With tDOC% (All N = 76, p < 0.05)

Optical property	Fitting formula	Parameter		Adjusted r^2	Consistent with river data[a]
		a	*b*		
a_{440} (m^{-1})	$y = a \times tDOC\% + b$	4.75×10^{-3}	3.08×10^{-2}	0.60	×
$S_{275-295}$ (nm^{-1})	$y = \exp(a \times tDOC\% + b)$	-8.52×10^{-3}	−3.59	0.55	√
S_R	$y = \exp(a \times tDOC\% + b)$	-1.06×10^{-2}	5.83×10^{-1}	0.55	√
$SUVA_{254}$ (L mg-C^{-1} m^{-1})	$y = a \times tDOC\% + b$	3.14×10^{-2}	7.86×10^{-1}	0.66	√
FI	$y = a \times tDOC\% + b$	-3.17×10^{-3}	1.62	0.45	√
HIX	$y = \exp(a \times tDOC\% + b)$	6.21×10^{-3}	-4.43×10^{-1}	0.62	×
C2-Fmax/DOC	$y = a \times tDOC\% + b$	1.07×10^{-5}	1.29×10^{-4}	0.64	√

[a]Consistency corresponds to whether the extrapolated relationship at 100% tDOC falls within the reference river data from Sarawak: √—falls in the range, ×—falls out of the range.

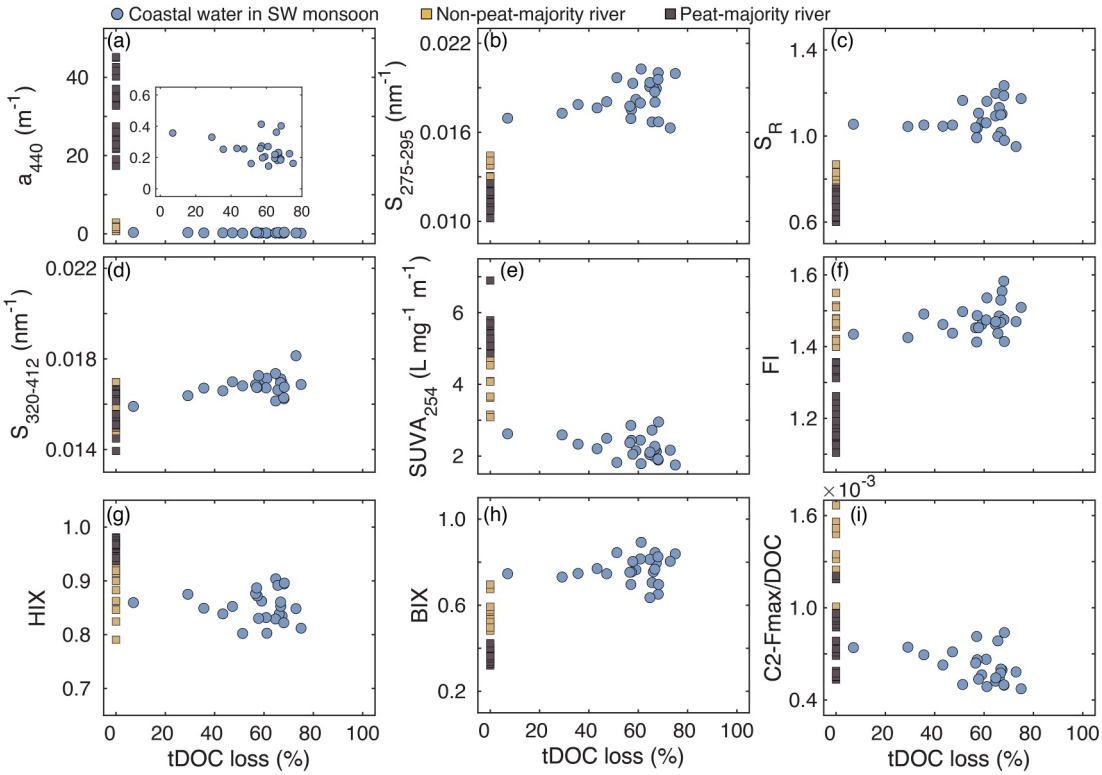

Figure 6. The relationship between optical properties and percentage terrestrial dissolved organic carbon (tDOC) remineralization (as calculated from the proportion of remineralized tDOC relative to total initial tDOC based on the carbon stable isotope mass balance). Coastal water data from the Singapore Strait are shown in blue circles (SW Monsoon season only) while Sarawak river data are showed in light and dark brown squares for rivers with, respectively, <50% (non-peat-majority river) and >50% (peat-majority river) peatland coverage in their catchments. We found no significant correlations for the Singapore data, indicating that these optical properties may not be able to quantify the extent of tDOC remineralization.

tDOC remineralization, if the denominator of total initial tDOC is also small, the inferred percentage tDOC remineralization can then vary erratically over a large range. We therefore excluded the data from the other seasons in which there is not a strong influence from peatland tDOC.

In contrast, most of the optical properties did show clear relationships to percentage tDOC loss in our laboratory photodegradation experiments, both with pure tDOC samples from a peatland-draining river (Maludam) and with coastal water samples from the Singapore Strait during the SW Monsoon (Figure 7). For Maludam river samples, CDOM a_{440} decreased linearly with tDOC loss while $S_{275–295}$ and S_R increased linearly by 64% and 156%, respectively (Figures 7a–7c). $S_{320–412}$ and $SUVA_{254}$ showed exponential decreases from ∼0.016 to ∼0.012 nm^{-1} and from ∼5.2 to ∼1.5 L mg-C^{-1} m^{-1}, respectively (Figures 7d and 7e). However, fluorescence properties showed more variability. FI first dropped by ∼10% upon 30%–40% tDOC loss, after which it increased (Figure 7f). HIX always stayed at around 0.93 across the whole percent tDOC loss (Figure 7g) and BIX started to rise once tDOC loss exceeded 50% (Figure 7h). C2-Fmax/DOC exhibited a general increase of more than two times of the initial value. For the two coastal water samples from Singapore, we estimated tDOC loss by taking the prior natural tDOC remineralization (from our isotope mass balance) into account, and we conservatively assumed that all DOC lost during the incubation was tDOC, because marine DOC at our site is not very photo-sensitive (Zhou et al., 2021). Although only little DOC was remineralized in the coastal water samples, $S_{275–295}$ and S_R changed by more than twofold relative to the initial values, while $SUVA_{254}$, HIX and C2-Fmax/DOC decreased linearly to a smaller degree with percent tDOC loss. $S_{320–412}$ and BIX only changed slightly.

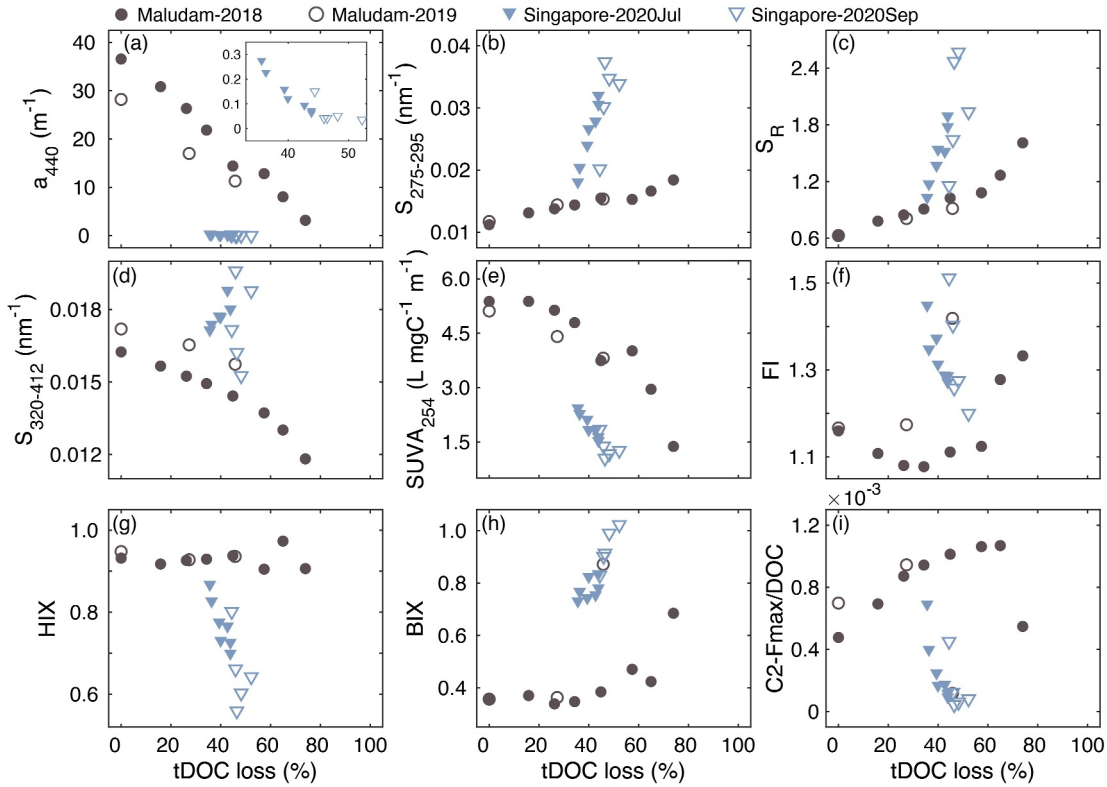

Figure 7. Changes in optical properties as a function of the percentage loss of terrestrial dissolved organic carbon (tDOC) during pure photodegradation experiments for Singapore coastal water and water from a peatland-draining river in Sarawak (Maludam River). Unlike the patterns of optical properties against percent tDOC loss in natural coastal water, most of the parameters did present certain correlations to tDOC loss in laboratory incubation purely under photo exposure, but the correlations were different for different water types. Shapes of symbols represent the experimental water sample, with circles representing river water (Maludam) and triangles representing coastal seawater (Singapore).

4. Discussion

4.1. Reliability of tDOC Calculation

Carbon stable isotope measurements can provide strong insights into sources and biogeochemical processing of DOM (Alling et al., 2008; Bauer & Bianchi, 2011; S. A. Lee et al., 2020). As DOM from terrestrial sources and marine environments possess distinctive carbon isotope compositions, the $\delta^{13}C_{DOC}$ values are widely used as fingerprints to distinguish DOC from different sources based on endmember mixing models (Humborg et al., 2017; Ye et al., 2018; Zhou et al., 2021). Our estimated endmember $\delta^{13}C_{DOC}$ values (Table S2 in Supporting Information S1) conform to the generally reported ranges of −25‰ to −32‰ and −21‰ to −22‰ for riverine and marine endmembers, respectively (Bauer, 2002; Beaupré, 2015; Gandois et al., 2014). From our estimated endmember values for $\delta^{13}C_{DOC}$ and the measured DOC concentrations in our coastal samples we could therefore use a mixing model to estimate the remaining tDOC concentration (Section 2.5.2 and Text S1.1 in Supporting Information S1).

Several previous studies have applied a stable carbon isotope mass balance approach to quantify the contribution of terrestrial organic matter degradation to the observed DIC and $\delta^{13}C_{DIC}$ in different regions (Humborg et al., 2017; Samanta et al., 2015; Su et al., 2020; Zhou et al., 2021). For example, it was estimated from the depletion in $\delta^{13}C_{DIC}$ that annually 4.0 Tg terrestrial organic matter is respired in the central and outer Laptev Sea in the Arctic (Humborg et al., 2017). Based on a compiled data set including DIC, $\delta^{13}C_{DIC}$, dissolved calcium and oxygen, it was found that remineralization is the main cause of the deviation from conservative mixing in the Hooghly River estuary in India (Samanta et al., 2015). Similarly, a mass balance calculation in the hypoxic zone of the Pearl River estuary in China demonstrated that on average 35% of the total organic matter remineralization was of terrestrial organic matter (Su et al., 2017), while in the Chesapeake Bay in the US, remineralization of autochthonous organic matter was the dominant oxygen-consuming process (Su et al., 2020). The deviation of

measured $\delta^{13}C_{DIC}$ from its conservative mixing value in our data set (around −1‰ during the SW Monsoon) is similar to the deviation observed in these previous studies, which suggests that our mass balance calculation provides robust estimates of tDOC remineralization.

The riverine DOC and CDOM endmember concentrations inferred from our analysis (Figure 3) can be considered to consist entirely of tDOC and terrigenous CDOM. The DOC concentration in these and other peat-draining rivers in Southeast Asia is linearly related to catchment peat coverage, indicating that peatlands are the main source of DOC in these rivers (Rixen et al., 2022). Blackwater rivers on Sumatra and Borneo also have low concentrations of nutrients (dissolved inorganic nitrogen often <15 μmol L^{-1}) and chlorophyll (<1 μg L^{-1}) (Bange et al., 2019; Baum & Rixen, 2014; Martin et al., 2018), and the extremely high concentrations of CDOM absorb most sunlight within a few tens of centimeters. These blackwater rivers also have notably low pH and oxygen concentrations, reaching hypoxic levels (Alkhatib et al., 2007; Bange et al., 2019; Rixen et al., 2008; Wit et al., 2015). Moreover, DOC accounts for >95% of the total organic carbon in these peatland-draining rivers (Baum et al., 2007; Moore et al., 2011; Müller et al., 2015), and hence terrestrial POC can only have at most a minor influence over the observed DIC and $\delta^{13}C_{DIC}$ in the water column.

4.2. Preferential Loss of CDOM Compared to tDOC During Natural Remineralization

tDOC generally has a high content of chromophores, and CDOM in estuaries and coastal waters is therefore often of terrestrial origin (Asmala et al., 2012; Z. Chen et al., 2015; Osburn et al., 2016; Santos et al., 2016). This characteristic provides the basis for using optical properties to study tDOC. Absorption coefficients (a_λ) often show strong correlations with bulk DOC concentrations in rivers, estuaries and coastal waters (Asmala et al., 2012; Fichot et al., 2016; Mann et al., 2016; Martin et al., 2018; Stedmon et al., 2011). However, we also observed preferential removal of CDOM compared to tDOC remineralization, although the difference was relatively modest (74% vs. 53% loss). This finding is consistent with previous work on biological and photochemical processes of DOM for freshwater (Benner & Kaiser, 2011; Martin et al., 2018; Spencer, Stubbins, et al., 2009) and coastal waters (Moran et al., 2000; Osburn et al., 2009). For example, the half-life time of CDOM in the Mackenzie River was estimated to be shorter than that of DOC when the river water was exposed to sunlight (Osburn et al., 2009). Similarly, removal of CDOM was found to be 21% more than that of DOC in biodegradation incubations conducted with water from a coastal estuary in Georgia after it was photo-exposed (Moran et al., 2000). Moreover, a large decrease in a_{355}/DOC ratio against salinity was observed in waters from the Middle Atlantic Bight, especially when the solar irradiance was higher (Del Vecchio & Blough, 2004b). A key mechanism driving preferential CDOM loss is likely that aromatic structures in chromophores can be partly oxidized to non-chromophoric DOC, especially by reactive oxygen species formed under photo exposure (Cory & Kling, 2018; Del Vecchio & Blough, 2002; Vione et al., 2009). Our finding that CDOM loss is greater than tDOC loss is therefore fully consistent with previous experimental and observational research in other regions.

Pure biodegradation of Southeast Asian peatland DOM appears to be too slow to account for the observed extent of remineralization (Nichols & Martin, 2021). A large fraction of this DOM is photolabile, yet the rate of pure photochemical degradation is also too low to explain the observed tDOC remineralization in this region (Zhou et al., 2023). This is consistent with the limited contribution of pure photochemical tDOC remineralization reported from other environments (Fichot & Benner, 2014; Osburn et al., 2009; Reader & Miller, 2012), even though the contribution of pure photochemical remineralization does appear to be higher in Southeast Asia than elsewhere (Zhou et al., 2023). Therefore, it is most likely that interactive photo-stimulated biodegradation plays an important role in tDOC remineralization and CDOM decomposition. Notably, although there is a large extent of tDOC and CDOM removal, the tDOC and CDOM concentrations still showed a pattern of conservative mixing at our study site. While this might appear to be contradictory, in fact this only indicates that physical mixing over the salinity range observed at our site occurs faster than the remineralization rate, and that the majority of the observed remineralization therefore takes place upstream of our sampling site.

4.3. Accuracy of Optical Properties as Quantitative Tracers of tDOC Content in Natural Water

DOM optical properties have been widely measured in estuarine and coastal environments, and it is clear that they can be sensitive indicators of the presence of tDOC (Fichot & Benner, 2012; Kaiser et al., 2017; Massicotte et al., 2017; Mizubayashi et al., 2013; Painter et al., 2018; Stedmon & Nelson, 2015). Several environmental studies have also demonstrated that some optical properties (a_λ and $S_{275–295}$) can be used to quantify tDOC

concentration as calculated from lignin phenols (Fichot & Benner, 2012; Fichot et al., 2016; Hernes & Benner, 2003; Lu et al., 2016; Walker et al., 2013). However, lignin phenols are a small (typically 0.1%–4% of DOC; Hernes et al., 2007; Opsahl & Benner, 1997; Osburn et al., 2016) and potentially rather labile (Benner & Kaiser, 2011; Cao et al., 2018; Hernes & Benner, 2003) fraction of tDOC, while terrigenous CDOM and FDOM may also be preferentially removed relative to bulk tDOC (Benner & Kaiser, 2011; Moran et al., 2000; Osburn et al., 2009). Specifically, both lignin and CDOM/FDOM are composed to a significant degree of aromatic moieties, which are especially photo-labile, while most aliphatic compounds are less susceptible to photo-degradation (Berggren et al., 2022; Opsahl & Benner, 1998; Osburn et al., 2001; Schmitt-Kopplin et al., 1998). In contrast, aromatic components are generally more recalcitrant to microbial processes (Kang & Mitchell, 2013). These differences in reactivity can likely account for preferential removal of lignin phenols and of CDOM/FDOM relative to the bulk tDOC. For example, it was reported that the removal of lignin phenols and CDOM was more than twice as high as the loss of DOC during combined photo- and bio-degradation of water from Broad River in South Carolina in the US (Benner & Kaiser, 2011). However, the degree to which optical properties are lost preferentially is likely dependent on the relative rates of different degradation processes, which are poorly quantified in natural environments. Therefore, it is still unclear how accurately these optical properties can trace total tDOC when it is also being subjected to natural remineralization processes. In the present study, we therefore used $\delta^{13}C_{DOC}$ to estimate tDOC concentration and $\delta^{13}C_{DIC}$ to estimate the extent of prior tDOC remineralization. Our results provide robust statistical evidence that all the optical properties typically used to identify tDOM are significantly related to tDOC% even when more than half of tDOC has already been remineralized (Figures 3 and 5). However, the different properties have variably strong relationships and differ in their sensitivity to tDOC in different parts of the tDOC% range.

The strong linear relationship between a_{440} and tDOC% shows that CDOM absorption coefficients can still be used to quantify tDOC in coastal water even when extensive remineralization has taken place. However, the fact that we did observe preferential removal of CDOM relative to tDOC (Figures 3e and 3f) underscores the fact that a_λ–tDOC relationships are sensitive to the extent of tDOM biogeochemical degradation and must therefore change significantly across estuarine and coastal gradients. In addition, the high variability of a_{440} in estuaries can result from the mixing of seawater and different rivers with highly distinctive concentrations of tDOC and CDOM depending on the catchment coverage of peatland (Rixen et al., 2022). Caution would therefore be needed in attempting to calculate tDOC concentrations from a_λ when the range in remineralization might be large and when the riverine influence is complex.

The non-linear relationships we observed for $S_{275–295}$ and S_R with tDOC% are consistent with previous studies showing exponential relationships for $S_{275–295}$ with lignin phenol concentration (Benner et al., 2005; Fichot & Benner, 2012) and linear correlation for S_R with carbon-normalized lignin yield (Spencer et al., 2010). Besides, after extrapolating the fitting curve to salinity 0, the relationships showed good consistency with tropical peatland river data, suggesting that unlike CDOM absorption, these spectral slope-based properties maintain a constant relationship to tDOC% even as tDOC is remineralized. Based on the r^2 and confidence intervals, both $S_{275–295}$ and S_R show similar accuracy for quantifying tDOC% (Figure 5 and Table 2), resulting from the relatively steady $S_{350–400}$ across the whole salinity gradient (data not shown), consistent with previous research (Fichot & Benner, 2012). It is interesting to note that compared to $S_{275–295}$, the slope ratio S_R shows less variability at mid-salinities in the data from Sarawak, suggesting that S_R might be less sensitive to the mixing among different rivers (Figure 4d). However, in our time series data from the Singapore Strait, $S_{275–295}$ and S_R are equally well related to tDOC% (Figure 5).

$SUVA_{254}$ is usually interpreted as a measure of DOM aromaticity, as shown by ^{13}C-NMR measurements with organic matter from a variety of aquatic environments (Weishaar et al., 2003). Moreover, $SUVA_{254}$ was recently proposed as a measure to distinguish between primarily photochemically labile tDOC and bio-labile tDOC in the UniDOM biogeochemical modeling framework (Anderson et al., 2019). Our study demonstrates that $SUVA_{254}$ is linearly related to tDOC% and performs better than other CDOM measures as a quantitative tDOC tracer, given that the relationship shows less scatter ($r^2 = 0.66$) and narrower confidence and prediction intervals (Figure 5e). This is consistent with the robust positive relationships between $SUVA_{254}$ and the fraction of humic substances obtained from a diverse range of watersheds in the US (Spencer et al., 2012). We note that our $SUVA_{254}$–tDOC% relationship extrapolates to the lower boundary of available river data. While the true $SUVA_{254}$ for rivers on Sumatra is not known, this result likely indicates some sensitivity of $SUVA_{254}$ to preferential CDOM loss during tDOC remineralization, which perhaps helps to explain some of the scatter in the relationship. $SUVA_{254}$ also

ignores absorption at longer wavelengths, which can include effects such as charge transfer (Y. Chen et al., 2020; Sharpless & Blough, 2014). Our data cannot confirm whether reduction in $SUVA_{254}$ reflects the conversion of primarily photo-labile tDOC to bio-labile structures as suggested in the UniDOM model (Anderson et al., 2019), but they do suggest that $SUVA_{254}$ can provide a good measure of tDOC in coastal environments.

The FI and HIX are also widely used as tDOC tracers but mainly as qualitative indicators. It is suggested that when FI is less than 1.4, the DOC pool is dominated by terrestrial matter, while FI larger than 1.4 indicates an increasing dominance of microbially-derived DOC (Cory et al., 2010; McKnight et al., 2001). Our data show that FI has a clear linear relationship with tDOC% (Figure 5f), which notably contrasts with the poor relationship between FI and the proportion of humic substances in DOM reported from a river basin in eastern Thailand (Kida et al., 2018). However, the formula of FI calculation is not strictly fixed, depending on how fluorescence spectral correction is conducted (Cory & McKnight, 2005; Cory et al., 2010; McKnight et al., 2001). Additionally, it has been suggested that FI changes by at least 0.1 units when there is a source change in DOM (McKnight et al., 2001). It is clear that FI can change up to 0.3 in the Singapore Strait over a range of tDOC% from 0 (during inter-monsoon seasons) to ∼60% (during the SW Monsoon). However, FI is also the most variable parameter in the river data, with some rivers having FI values similar to the inter-monsoon data from the Singapore Strait, despite carrying predominantly tDOC (Zhou et al., 2019). FI is therefore potentially less useful as a tDOC tracer than the other optical properties.

It is expected that HIX rises along with tDOC% increase because it indicates humification level, and humic substances are an important component of tDOC (Ohno, 2002; Zsolnay et al., 1999). However, similar to FI, the HIX calculation is not identical in different studies (Birdwell & Engel, 2010; Inamdar et al., 2011; M.-H. Lee et al., 2018; Ohno, 2002). We choose to use the formula after inner-filtering correction (Ohno, 2002) as our data set spans a large range of DOC concentrations. HIX does show a clear relationship with tDOC%, but notably, the river data do not fall on the same relationship extrapolated from the coastal water data. It is well known that humic substances can be broken down after tDOC experiences biogeochemical processes, reducing the humification level (Catalán et al., 2013; Hansen et al., 2016; Huguet et al., 2009; Wilske et al., 2020). Nevertheless, some studies also report that DOM can be transformed to humified materials under photo-exposure or during microbial degradation, thus causing HIX to increase (M. Chen & Jaffé, 2014; Garcia et al., 2018; Hansen et al., 2016; Kieber et al., 1997; Ortega-Retuerta et al., 2010). The complex changing patterns during biogeochemical processes may make HIX insensitive above a certain level of humification or tDOC%. For example, we note that HIX showed almost no change during photo-exposure of the Maludam River samples (Figure 7g).

We additionally consider C2-Fmax/DOC, as it was used previously to estimate tDOC% for the Sarawak data, assuming that there would be no preferential removal of C2 relative to bulk tDOC over the small spatial scales of the estuaries in Sarawak (Zhou et al., 2019). Our new data from Singapore correspond to a longer water residence time, providing more opportunity for preferential removal of C2, which is expected to be fairly photo-labile (Grunert et al., 2021; Sankar et al., 2019). Some other studies have investigated relationships between absolute Fmax values and tDOC tracers such as lignin phenols (Osburn & Stedmon, 2011; Walker et al., 2013; Yang & Hur, 2014). However, given the substantial physical dilution of riverine tDOC and FDOM across a salinity range from freshwater to salinity >25, DOC normalization is appropriate. C2-Fmax/DOC is thus analogous to $SUVA_{254}$. Our data confirm that this measure is able to quantify tDOC% nearly as well as $SUVA_{254}$ across the large range (0%–60%) seen in our Singapore Strait data, with a strong correlation coefficient (r^2 = 0.64, Figure 5i). This agrees with the strong linear correlation of C2 fluorescence to concentrations of lignin phenols obtained from Arctic rivers (Walker et al., 2013).

In contrast to these optical measures associated with tDOC, neither $S_{320–412}$ nor BIX were related to tDOC%, and indeed showed little variation throughout our time series. The Singapore Strait does not appear to experience large seasonality in phytoplankton production, with chlorophyll concentrations mostly <2 μg L^{-1} (Martin et al., 2022), and the production and microbial processing of autochthonous DOC are likely closely coupled year-round, with a relatively refractory marine DOC pool (Zhou et al., 2021). While our data thus cannot evaluate how well these two optical properties can trace the presence of freshly produced autochthonous DOC, our results do show that in the absence of large changes in fresh autochthonous DOC inputs (Martin et al., 2022), they show fairly stable values even as the DOC pool receives highly variable amounts of additional tDOC input (Figures 1f and 2e). Interestingly, $S_{320–412}$ and BIX were not correlated with each other or with chlorophyll-a concentration (Figure S6 in Supporting Information S1), but given the low variability in all three variables this result is not surprising.

Overall, our data thus demonstrate that all optical properties that are typically associated with tDOC (a_{440}, $S_{275–295}$, S_R, $SUVA_{254}$, FI, HIX, and C2-Fmax/DOC) are indeed quantitatively related to tDOC% in coastal water, even after the tDOC has undergone a substantial degree of remineralization. However, the optical properties differ in the shape of the relationship to tDOC%, indicating differences in applicability. $S_{275–295}$, S_R and HIX show non-linear change with tDOC%, which makes them very sensitive to small changes in tDOC concentration at low tDOC%, but much less sensitive to tDOC% above a certain level (~40%–60%). On the other hand, a_{440}, $SUVA_{254}$, FI and C2-Fmax/DOC present linear behaviors. This means that they are less sensitive than the non-linear-related indicators at low tDOC%, but they show a consistent ability to quantify tDOC% at least within the range of 0%–60%. Clearly, however, the preferential removal of CDOM means that a_λ needs to be used cautiously to quantify tDOC if the range in possible remineralization extent is large. The fact that $SUVA_{254}$ and C2-Fmax/DOC are normalized to DOC concentration appears to make these measures more robust, although the need for DOC measurements makes these parameters less easy and less rapid to measure. Thus, it is essential to understand basic characteristics of certain water samples and consider measurement limitations before choosing appropriate optical indicators to quantify tDOC%.

4.4. Qualitative Proxies of tDOC Biogeochemical Processes

Our carbon stable isotope mass balance shows clearly that a variable proportion of the original tDOC was remineralized before reaching our site. It has previously been demonstrated that biodegradation and UV irradiation can cause optical properties to change in different directions and/or at different rates (Hansen et al., 2016; Helms et al., 2008; M.-H. Lee et al., 2018). Subsequently, such changes might allow one to use optical properties to diagnose certain biogeochemical processes: for example, photochemical and microbial degradation of tDOC are reported to affect S_R differently (Hansen et al., 2016; Helms et al., 2008), while photochemical degradation consistently increases $S_{275–295}$ (Fichot & Benner, 2012; Helms et al., 2014; Zhou et al., 2021). Here, we additionally tested whether the optical properties can also be used to infer the extent of natural tDOC remineralization in the natural environment. However, unlike the strong relationships to tDOC%, and despite spanning a range of 20%–80% tDOC loss, none of the optical properties showed any consistent trends with tDOC loss (Figure 6).

The fact that the optical properties show little change with tDOC loss percentage could arise from the complexity of biogeochemical processes in the natural environment, where photodegradation, biodegradation, and their interactions take place simultaneously and coastal mixing occurs (Del Vecchio & Blough, 2002; Fovet et al., 2020; Lønborg et al., 2010; Osburn et al., 2009; Ward et al., 2017). Generally, photodegradation is considered to play a significant role in tDOC remineralization. Yet, the extent and rate of photo-induced remineralization and optical property change can vary depending on light intensities, irradiation wavelengths and specific origins of tDOC (Clark et al., 2020; Du et al., 2016; Hansen et al., 2016; M.-H. Lee et al., 2018; Moran et al., 2000). It has been shown that biodegradation may cause optical properties of DOM to change less and possibly in an opposite direction compared to photodegradation (Hansen et al., 2016; Hernes & Benner, 2003; Hur et al., 2011; M.-H. Lee et al., 2018). Microbial remineralization of tDOC is often significantly enhanced after partial photodegradation (Hansen et al., 2016; Miller & Moran, 1997; Moran et al., 2000), but conversely, photochemical reactions can also compete with microbial processes (Amado et al., 2015; Ward et al., 2017). In natural coastal environments, photo-induced reactions and microbial remineralization most likely always co-occur and interact at least to some degree. It is therefore possible that different co-occurring remineralization processes result in more limited changes in optical properties than those observed in single-process incubation experiments. A recent experimental study showed that microbial and combined photochemical + microbial degradation caused the optical properties of different plant leachates to converge over time despite large differences in initial properties (Harfmann et al., 2019). Tropical peatland tDOM experiences partial degradation within the peat dome before entering rivers (Gandois et al., 2014), so it is possible that the optical properties of the riverine tDOM pool have already undergone "microbial buffering" (Harfmann et al., 2019). Subsequent interactive photochemical and microbial degradation might then only have a limited impact on CDOM and FDOM spectral characteristics, consistent with our observations.

In the case of riverine tDOC from Southeast Asian peatlands, pure microbial remineralization appears to be relatively slow and no clear alteration of optical properties was found in microbial incubation experiments of 3–6 months duration (Nichols & Martin, 2021; Zhou et al., 2021). We therefore compare our environmental data to results from pure photodegradation experiments. For most parameters, especially $S_{275–295}$, S_R, and $SUVA_{254}$, we observed clear changes with consistent direction (i.e., increasing or decreasing) as a function of tDOC loss

percentage for both the peatland-draining river samples and the coastal water samples, and these changes are consistent with those reported previously for tDOM photobleaching experiments (Du et al., 2016; Helms et al., 2013; M.-H. Lee et al., 2018; Magyan & Dempsey, 2021). Notably, we observed that the coastal water samples mostly showed much more obvious changes in optical properties for a given %tDOC loss than the river samples. The different rates of change are to be expected because coastal water samples contain overall less CDOM and FDOM, and consist of a mixture of marine and terrestrial DOM, while the river samples still consisted of tDOM even at the end of the incubations. The results of bio- and photo-incubation for water from the peatland-draining river suggest that Southeast Asian peatland-derived tDOM behaves similar to other highly humified photo-labile but bio-refractory tDOM during remineralization (M. Chen & Jaffé, 2014; Dempsey et al., 2020). The fact that our environmental data do not demonstrate such clear relationships between optical properties and tDOC loss therefore suggests that natural tDOC remineralization in this region proceeds through complex interactive degradation processes that do not leave clear signatures in a single optical property. More degradation experiments are therefore needed to reveal whether these optical properties can be used in combination to distinguish specific biogeochemical processes in the natural coastal water as M.-H. Lee et al. (2018) did for DOM from certain sources. It would also be especially valuable for further research to examine how simultaneous photo- and biodegradation of tDOM alter its optical properties, as both processes would take place simultaneously in the natural environment.

5. Conclusions

In summary, our study shows that there is preferential removal of optically active tDOM relative to total tDOC, but that DOM optical properties are nevertheless robust and potentially quantitative indicators of tDOC% in coastal waters. The commonly used optical properties a_{440}, $S_{275–295}$, S_R, $SUVA_{254}$, FI, and HIX, as well as C2-Fmax/DOC, can all quantify tDOC% in coastal water, but their relationships with tDOC% exhibit different shapes, accuracies and applicable ranges. Specifically, CDOM spectral slope parameters are very sensitive to the presence of low levels of tDOC, but show little further change once tDOC exceeds ∼40% of total DOC. In contrast, $SUVA_{254}$ and C2-Fmax/DOC show linear relationships with tDOC contribution across a larger range of values. However, none of the optical properties we considered show a relationship to the extent of tDOC remineralization, which we attribute to the likely complexity of multiple interacting biogeochemical degradation processes in the natural environment.

Data Availability Statement

Processed data are available in Data Set S1. The data that support the findings of this study (Y. Chen et al., 2023) are openly available in Nanyang Technological University Data Repository at https://doi.org/10.21979/N9/Q1L9HR.

Acknowledgments
We thank Oon Yee Woo, Su Ping Heng, Kristy Y.W. Chang, Ashleen S.Y. Tan, Molly A. Moynihan, Robert S. Nichols, and Nikita Kaushal for help with field sampling and laboratory analysis, and the captains and crew of *Dolphin Explorer* and R/V *Galaxea* for support in the field. We are grateful to Richard Sanders for comments that helped to guide the analysis. This research was funded by the Singapore Ministry of Education through Academic Research Fund Tier 2 Grant MOE-MOET2EP10121-0007 and by the National Research Foundation, Singapore, Prime Minister's Office through Grants MSRDP-P32 and NRF-NRI-2020-MESN. Permission for this research was given by the National Parks Board, Singapore, under permit NPRP17-044.

References

Aksnes, D. L., Dupont, N., Staby, A., Fiksen, Ø., Kaartvedt, S., & Aure, J. (2009). Coastal water darkening and implications for mesopelagic regime shifts in Norwegian fjords. *Marine Ecology Progress Series*, *387*, 39–49. https://doi.org/10.3354/meps08120

Alkhatib, M., Jennerjahn, T. C., & Samiaji, J. (2007). Biogeochemistry of the Dumai River estuary, Sumatra, Indonesia, a tropical black-water river. *Limnology and Oceanography*, *52*(6), 2410–2417. https://doi.org/10.4319/lo.2007.52.6.2410

Alling, V., Humborg, C., Mörth, C.-M., Rahm, L., & Pollehne, F. (2008). Tracing terrestrial organic matter by $\delta^{34}S$ and $\delta^{13}C$ signatures in a subarctic estuary. *Limnology and Oceanography*, *53*(6), 2594–2602. https://doi.org/10.4319/lo.2008.53.6.2594

Alling, V., Porcelli, D., Mörth, C. M., Anderson, L., Sanchez-Garcia, L., Gustafsson, Ö., et al. (2012). Degradation of terrestrial organic carbon, primary production and out-gassing of CO_2 in the Laptev and East Siberian Seas as inferred from $\delta^{13}C$ values of DIC. *Geochimica et Cosmochimica Acta*, *95*, 143–159. https://doi.org/10.1016/j.gca.2012.07.028

Amado, A. M., Cotner, J. B., Cory, R. M., Edhlund, B. L., & McNeill, K. (2015). Disentangling the interactions between photochemical and bacterial degradation of dissolved organic matter: Amino acids play a central role. *Microbial Ecology*, *69*(3), 554–566. https://doi.org/10.1007/s00248-014-0512-4

Anderson, T. R., Rowe, E. C., Polimene, L., Tipping, E., Evans, C. D., Barry, C. D. G., et al. (2019). Unified concepts for understanding and modelling turnover of dissolved organic matter from freshwaters to the ocean: The UniDOM model. *Biogeochemistry*, *146*(2), 105–123. https://doi.org/10.1007/s10533-019-00621-1

Antony, R., Willoughby, A. S., Grannas, A. M., Catanzano, V., Sleighter, R. L., Thamban, M., & Hatcher, P. G. (2018). Photo-biochemical transformation of dissolved organic matter on the surface of the coastal East Antarctic ice sheet. *Biogeochemistry*, *141*(2), 229–247. https://doi.org/10.1007/s10533-018-0516-0

Asmala, E., Stedmon, C. A., & Thomas, D. N. (2012). Linking CDOM spectral absorption to dissolved organic carbon concentrations and loadings in boreal estuaries. *Estuarine, Coastal and Shelf Science*, *111*, 107–117. https://doi.org/10.1016/j.ecss.2012.06.015

Bange, H. W., Sim, C. H., Bastian, D., Kallert, J., Kock, A., Mujahid, A., & Müller, M. (2019). Nitrous oxide (N_2O) and methane (CH_4) in rivers and estuaries of northwestern Borneo. *Biogeosciences*, *16*(22), 4321–4335. https://doi.org/10.5194/bg-16-4321-2019

Bauer, J. E. (2002). Chapter 8 - Carbon isotopic composition of DOM. In D. A. Hansell & C. A. Carlson (Eds.), *Biogeochemistry of marine dissolved organic matter* (pp. 405–453). Academic Press. https://doi.org/10.1016/B978-012323841-2/50010-5

Bauer, J. E., & Bianchi, T. S. (2011). 5.02 - Dissolved organic carbon cycling and transformation. In E. Wolanski & D. McLusky (Eds.), *Treatise on estuarine and coastal science* (pp. 7–67). Academic Press. https://doi.org/10.1016/B978-0-12-374711-2.00502-7

Baum, A., & Rixen, T. (2014). Dissolved inorganic nitrogen and phosphate in the human affected blackwater river Siak, central Sumatra, Indonesia. *Asian Journal of Water, Environment and Pollution*, *11*, 13–24.

Baum, A., Rixen, T., & Samiaji, J. (2007). Relevance of peat draining rivers in central Sumatra for the riverine input of dissolved organic carbon into the ocean. *Estuarine, Coastal and Shelf Science*, *73*(3), 563–570. https://doi.org/10.1016/j.ecss.2007.02.012

Beaupré, S. R. (2015). Chapter 6 - The carbon isotopic composition of marine DOC. In D. A. Hansell & C. A. Carlson (Eds.), *Biogeochemistry of marine dissolved organic matter* (2nd ed., pp. 335–368). Academic Press. https://doi.org/10.1016/B978-0-12-405940-5.00006-6

Bélanger, S., Xie, H., Krotkov, N., Larouche, P., Vincent, W. F., & Babin, M. (2006). Photomineralization of terrigenous dissolved organic matter in Arctic coastal waters from 1979 to 2003: Interannual variability and implications of climate change. *Global Biogeochemical Cycles*, *20*(4), GB4005. https://doi.org/10.1029/2006GB002708

Beleites, C., & Sergo, V. (2018). hyperSpec: A package to handle hyperspectral data sets in R. R package version 0.99-20180627. Retrieved from http://hyperspec.r-forge.r-project.org

Benner, R., & Kaiser, K. (2011). Biological and photochemical transformations of amino acids and lignin phenols in riverine dissolved organic matter. *Biogeochemistry*, *102*(1), 209–222. https://doi.org/10.1007/s10533-010-9435-4

Benner, R., Louchouarn, P., & Amon, R. M. W. (2005). Terrigenous dissolved organic matter in the Arctic Ocean and its transport to surface and deep waters of the North Atlantic. *Global Biogeochemical Cycles*, *19*(2), GB2025. https://doi.org/10.1029/2004GB002398

Berggren, M., Guillemette, F., Bieroza, M., Buffam, I., Deininger, A., Hawkes, J. A., et al. (2022). Unified understanding of intrinsic and extrinsic controls of dissolved organic carbon reactivity in aquatic ecosystems. *Ecology*, *103*(9), e3763. https://doi.org/10.1002/ecy.3763

Birdwell, J. E., & Engel, A. S. (2010). Characterization of dissolved organic matter in cave and spring waters using UV–Vis absorbance and fluorescence spectroscopy. *Organic Geochemistry*, *41*(3), 270–280. https://doi.org/10.1016/j.orggeochem.2009.11.002

Boutton, T. W. (1991). *Stable carbon isotope ratios of natural materials: 2 Atmospheric, terrestrial, marine, and freshwater environments*. Academic Press, Inc. Retrieved from http://inis.iaea.org/search/search.aspx?orig_q=RN:24010391

Bushaw-Newton, K. L., & Moran, M. A. (1999). Photochemical formation of biologically available nitrogen from dissolved humic substances in coastal marine systems. *Aquatic Microbial Ecology*, *18*(3), 285–292. https://doi.org/10.3354/ame018285

Cao, X., Aiken, G. R., Butler, K. D., Huntington, T. G., Balch, W. M., Mao, J., & Schmidt-Rohr, K. (2018). Evidence for major input of riverine organic matter into the ocean. *Organic Geochemistry*, *116*, 62–76. https://doi.org/10.1016/j.orggeochem.2017.11.001

Capelle, D. W., Kuzyk, Z. Z. A., Papakyriakou, T., Guéguen, C., Miller, L. A., & Macdonald, R. W. (2020). Effect of terrestrial organic matter on ocean acidification and CO_2 flux in an Arctic shelf sea. *Progress in Oceanography*, *185*, 102319. https://doi.org/10.1016/j.pocean.2020.102319

Cartisano, C. M., Del Vecchio, R., Bianca, M. R., & Blough, N. V. (2018). Investigating the sources and structure of chromophoric dissolved organic matter (CDOM) in the North Pacific Ocean (NPO) utilizing optical spectroscopy combined with solid phase extraction and borohydride reduction. *Marine Chemistry*, *204*, 20–35. https://doi.org/10.1016/j.marchem.2018.05.005

Catalán, N., Obrador, B., Felip, M., & Pretus, J. L. (2013). Higher reactivity of allochthonous vs. autochthonous DOC sources in a shallow lake. *Aquatic Sciences*, *75*(4), 581–593. https://doi.org/10.1007/s00027-013-0302-y

Chen, M., & Jaffé, R. (2014). Photo- and bio-reactivity patterns of dissolved organic matter from biomass and soil leachates and surface waters in a subtropical wetland. *Water Research*, *61*, 181–190. https://doi.org/10.1016/j.watres.2014.03.075

Chen, Y., Liu, J., Zhang, X., & Blough, N. V. (2020). Time-resolved fluorescence spectra of untreated and sodium borohydride-reduced chromophoric dissolved organic matter. *Environmental Science & Technology*, *54*(19), 12109–12118. https://doi.org/10.1021/acs.est.0c03135

Chen, Y., Martin, P., & Zhou, Y. (2023). Replication data for: The validity of optical properties as tracers of terrigenous dissolved organic carbon during extensive remineralization in coastal waters [Dataset]. *DR-NTU (Data)*. https://doi.org/10.21979/N9/Q1L9HR

Chen, Z., Doering, P. H., Ashton, M., & Orlando, B. A. (2015). Mixing behavior of colored dissolved organic matter and its potential ecological implication in the Caloosahatchee River Estuary, Florida. *Estuaries and Coasts*, *38*(5), 1706–1718. https://doi.org/10.1007/s12237-014-9916-0

Cheng, L., Normandeau, C., Bowden, R., Doucett, R., Gallagher, B., Gillikin, D. P., et al. (2019). An international intercomparison of stable carbon isotope composition measurements of dissolved inorganic carbon in seawater. *Limnology and Oceanography: Methods*, *17*(3), 200–209. https://doi.org/10.1002/lom3.10300

Chin, Y.-P., Aiken, G., & O'Loughlin, E. (1994). Molecular weight, polydispersity, and spectroscopic properties of aquatic humic substances. *Environmental Science & Technology*, *28*(11), 1853–1858. https://doi.org/10.1021/es00060a015

Ciais, P., Sabine, C., Bala, G., & Peters, W. (2013). Carbon and other biogeochemical cycles. In T. F. Stocker, D. Qin, G. K. Plattner, M. Tignor, S. K. Allen, J. Boschung, et al. (Eds.), *Climate change 2013: The physical science basis. Contribution of Working Group I to the fifth assessment report of the Intergovernmental Panel on Climate Change* (pp. 465–570). Cambridge University Press. Retrieved from https://edepot.wur.nl/345905

Clark, C. D., De Bruyn, W. J., Brahm, B., & Aiona, P. (2020). Optical properties of chromophoric dissolved organic matter (CDOM) and dissolved organic carbon (DOC) levels in constructed water treatment wetland systems in southern California, USA. *Chemosphere*, *247*, 125906. https://doi.org/10.1016/j.chemosphere.2020.125906

Coble, P. G. (1996). Characterization of marine and terrestrial DOM in seawater using excitation-emission matrix spectroscopy. *Marine Chemistry*, *51*(4), 325–346. https://doi.org/10.1016/0304-4203(95)00062-3

Coble, P. G. (2007). Marine optical biogeochemistry: The chemistry of ocean color. *Chemical Reviews*, *107*(2), 402–418. https://doi.org/10.1021/cr050350+

Cory, R. M., & Kling, G. W. (2018). Interactions between sunlight and microorganisms influence dissolved organic matter degradation along the aquatic continuum. *Limnology and Oceanography Letters*, *3*(3), 102–116. https://doi.org/10.1002/lol2.10060

Cory, R. M., & McKnight, D. M. (2005). Fluorescence spectroscopy reveals ubiquitous presence of oxidized and reduced quinones in dissolved organic matter. *Environmental Science & Technology*, *39*(21), 8142–8149. https://doi.org/10.1021/es0506962

Cory, R. M., Miller, M. P., McKnight, D. M., Guerard, J. J., & Miller, P. L. (2010). Effect of instrument-specific response on the analysis of fulvic acid fluorescence spectra. *Limnology and Oceanography: Methods*, *8*(2), 67–78. https://doi.org/10.4319/lom.2010.8.67

Dai, M., Yin, Z., Meng, F., Liu, Q., & Cai, W. J. (2012). Spatial distribution of riverine DOC inputs to the ocean: An updated global synthesis. *Current Opinion in Environmental Sustainability*, *4*(2), 170–178. https://doi.org/10.1016/j.cosust.2012.03.003

Danhiez, F. P., Vantrepotte, V., Cauvin, A., Lebourg, E., & Loisel, H. (2017). Optical properties of chromophoric dissolved organic matter during a phytoplankton bloom. Implication for DOC estimates from CDOM absorption. *Limnology and Oceanography*, *62*(4), 1409–1425. https://doi.org/10.1002/lno.10507

Del Vecchio, R., & Blough, N. V. (2002). Photobleaching of chromophoric dissolved organic matter in natural waters: Kinetics and modeling. *Marine Chemistry*, *78*(4), 231–253. https://doi.org/10.1016/S0304-4203(02)00036-1

Del Vecchio, R., & Blough, N. V. (2004a). On the origin of the optical properties of humic substances. *Environmental Science & Technology*, *38*(14), 3885–3891. https://doi.org/10.1021/es049912h

Del Vecchio, R., & Blough, N. V. (2004b). Spatial and seasonal distribution of chromophoric dissolved organic matter and dissolved organic carbon in the Middle Atlantic Bight. *Marine Chemistry*, *89*(1), 169–187. https://doi.org/10.1016/j.marchem.2004.02.027

Dempsey, C. M., Brentrup, J. A., Magyan, S., Knoll, L. B., Swain, H. M., Gaiser, E. E., et al. (2020). The relative importance of photodegradation and biodegradation of terrestrially derived dissolved organic carbon across four lakes of differing trophic status. *Biogeosciences*, *17*(24), 6327–6340. https://doi.org/10.5194/bg-17-6327-2020

Dittmar, T. (2015). Chapter 7 - Reasons behind the long-term stability of dissolved organic matter. In D. A. Hansell & C. A. Carlson (Eds.), *Biogeochemistry of Marine dissolved organic matter* (2nd ed., pp. 369–388). Academic Press. https://doi.org/10.1016/B978-0-12-405940-5.00007-8

Du, Y., Zhang, Y., Chen, F., Chang, Y., & Liu, Z. (2016). Photochemical reactivities of dissolved organic matter (DOM) in a sub-alpine lake revealed by EEM-PARAFAC: An insight into the fate of allochthonous DOM in alpine lakes affected by climate change. *Science of the Total Environment*, *568*, 216–225. https://doi.org/10.1016/j.scitotenv.2016.06.036

Evans, C. D., Page, S. E., Jones, T., Moore, S., Gauci, V., Laiho, R., et al. (2014). Contrasting vulnerability of drained tropical and high-latitude peatlands to fluvial loss of stored carbon. *Global Biogeochemical Cycles*, *28*(11), 1215–1234. https://doi.org/10.1002/2013GB004782

Fichot, C. G., & Benner, R. (2011). A novel method to estimate DOC concentrations from CDOM absorption coefficients in coastal waters. *Geophysical Research Letters*, *38*(3), n/a. https://doi.org/10.1029/2010gl046152

Fichot, C. G., & Benner, R. (2012). The spectral slope coefficient of chromophoric dissolved organic matter (S275–295) as a tracer of terrigenous dissolved organic carbon in river-influenced ocean margins. *Limnology and Oceanography*, *57*(5), 1453–1466. https://doi.org/10.4319/lo.2012.57.5.1453

Fichot, C. G., & Benner, R. (2014). The fate of terrigenous dissolved organic carbon in a river-influenced ocean margin. *Global Biogeochemical Cycles*, *28*(3), 300–318. https://doi.org/10.1002/2013GB004670

Fichot, C. G., Benner, R., Kaiser, K., Shen, Y., Amon, R. M. W., Ogawa, H., & Lu, C. J. (2016). Predicting dissolved lignin phenol concentrations in the coastal ocean from chromophoric dissolved organic matter (CDOM) absorption coefficients [Original Research]. *Frontiers in Marine Science*, *3*, 7. https://doi.org/10.3389/fmars.2016.00007

Fovet, O., Cooper, D. M., Jones, D. L., Jones, T. G., & Evans, C. D. (2020). Dynamics of dissolved organic matter in headwaters: Comparison of headwater streams with contrasting DOM and nutrient composition. *Aquatic Sciences*, *82*(2), 29. https://doi.org/10.1007/s00027-020-0704-6

Fry, B., & Sherr, E. B. (1989). $\delta^{13}C$ measurements as indicators of carbon flow in marine and freshwater ecosystems. In P. W. Rundel, J. R. Ehleringer, & K. A. Nagy (Eds.), *Stable isotopes in ecological research*.

Gandois, L., Teisserenc, R., Cobb, A. R., Chieng, H., Lim, L., Kamariah, A., et al. (2014). Origin, composition, and transformation of dissolved organic matter in tropical peatlands. *Geochimica et Cosmochimica Acta*, *137*, 35–47. https://doi.org/10.1016/j.gca.2014.03.012

Garcia, R. D., Diéguez, M. D. C., Gerea, M., Garcia, P. E., & Reissig, M. (2018). Characterisation and reactivity continuum of dissolved organic matter in forested headwater catchments of Andean Patagonia. *Freshwater Biology*, *63*(9), 1049–1062. https://doi.org/10.1111/fwb.13114

Gran, G. (1952). Determination of the equivalence point in potentiometric titrations. Part II. *The Analyst*, *77*(920), 661. https://doi.org/10.1039/an9527700661

Green, S. A., & Blough, N. V. (1994). Optical absorption and fluorescence properties of chromophoric dissolved organic matter in natural waters. *Limnology and Oceanography*, *39*(8), 1903–1916. https://doi.org/10.4319/lo.1994.39.8.1903

Grunert, B. K., Tzortziou, M., Neale, P., Menendez, A., & Hernes, P. (2021). DOM degradation by light and microbes along the Yukon River-coastal ocean continuum. *Scientific Reports*, *11*(1), 10236. https://doi.org/10.1038/s41598-021-89327-9

Han, H., Hwang, J., & Kim, G. (2021). Characterizing the origins of dissolved organic carbon in coastal seawater using stable carbon isotope and light absorption characteristics. *Biogeosciences*, *18*(5), 1793–1801. https://doi.org/10.5194/bg-18-1793-2021

Hansen, A. M., Kraus, T. E. C., Pellerin, B. A., Fleck, J. A., Downing, B. D., & Bergamaschi, B. A. (2016). Optical properties of dissolved organic matter (DOM): Effects of biological and photolytic degradation. *Limnology and Oceanography*, *61*(3), 1015–1032. https://doi.org/10.1002/lno.10270

Harfmann, J. L., Guillemette, F., Kaiser, K., Spencer, R. G. M., Chuang, C., & Hernes, P. J. (2019). Convergence of terrestrial dissolved organic matter composition and the role of microbial buffering in aquatic ecosystems. *Journal of Geophysical Research: Biogeosciences*, *124*(10), 3125–3142. https://doi.org/10.1029/2018JG004997

Harun, S., Baker, A., Bradley, C., & Pinay, G. (2016). Spatial and seasonal variations in the composition of dissolved organic matter in a tropical catchment: The Lower Kinabatangan River, Sabah, Malaysia. *Environmental Science: Processes & Impacts*, *18*(1), 137–150. https://doi.org/10.1039/C5EM00462D

Hedges, J. I., Keil, R. G., & Benner, R. (1997). What happens to terrestrial organic matter in the ocean? *Organic Geochemistry*, *27*(5), 195–212. https://doi.org/10.1016/S0146-6380(97)00066-1

Helms, J. R., Mao, J., Stubbins, A., Schmidt-Rohr, K., Spencer, R. G. M., Hernes, P. J., & Mopper, K. (2014). Loss of optical and molecular indicators of terrigenous dissolved organic matter during long-term photobleaching. *Aquatic Sciences*, *76*(3), 353–373. https://doi.org/10.1007/s00027-014-0340-0

Helms, J. R., Stubbins, A., Perdue, E. M., Green, N. W., Chen, H., & Mopper, K. (2013). Photochemical bleaching of oceanic dissolved organic matter and its effect on absorption spectral slope and fluorescence. *Marine Chemistry*, *155*, 81–91. https://doi.org/10.1016/j.marchem.2013.05.015

Helms, J. R., Stubbins, A., Ritchie, J. D., Minor, E. C., Kieber, D. J., & Mopper, K. (2008). Absorption spectral slopes and slope ratios as indicators of molecular weight, source, and photobleaching of chromophoric dissolved organic matter. *Limnology and Oceanography*, *53*(3), 955–969. https://doi.org/10.4319/lo.2008.53.3.0955

Hernes, P. J., & Benner, R. (2003). Photochemical and microbial degradation of dissolved lignin phenols: Implications for the fate of terrigenous dissolved organic matter in marine environments. *Journal of Geophysical Research*, *108*(C9), 3291. https://doi.org/10.1029/2002jc001421

Hernes, P. J., Robinson, A. C., & Aufdenkampe, A. K. (2007). Fractionation of lignin during leaching and sorption and implications for organic matter "freshness". *Geophysical Research Letters*, *34*(17), L17401. https://doi.org/10.1029/2007GL031017

Huang, T. H., Chen, C. T. A., Tseng, H. C., Lou, J. Y., Wang, S. L., Yang, L., et al. (2017). Riverine carbon fluxes to the South China Sea. *Journal of Geophysical Research: Biogeosciences*, *122*(5), 1239–1259. https://doi.org/10.1002/2016JG003701

Huguet, A., Vacher, L., Relexans, S., Saubusse, S., Froidefond, J., & Parlanti, E. (2009). Properties of fluorescent dissolved organic matter in the Gironde Estuary. *Organic Geochemistry*, *40*(6), 706–719. https://doi.org/10.1016/j.orggeochem.2009.03.002

Humborg, C., Geibel, M. C., Anderson, L. G., Björk, G., Mörth, C., Sundbom, M., et al. (2017). Sea-air exchange patterns along the central and outer East Siberian Arctic Shelf as inferred from continuous CO_2, stable isotope, and bulk chemistry measurements. *Global Biogeochemical Cycles*, *31*(7), 1173–1191. https://doi.org/10.1002/2017GB005656

Hur, J., Jung, K.-Y., & Schlautman, M. A. (2011). Altering the characteristics of a leaf litter-derived humic substance by adsorptive fractionation versus simulated solar irradiation. *Water Research*, *45*(18), 6217–6226. https://doi.org/10.1016/j.watres.2011.09.023

Hur, J., Williams, M. A., & Schlautman, M. A. (2006). Evaluating spectroscopic and chromatographic techniques to resolve dissolved organic matter via end member mixing analysis. *Chemosphere*, *63*(3), 387–402. https://doi.org/10.1016/j.chemosphere.2005.08.069

Inamdar, S., Singh, S., Dutta, S., Levia, D., Mitchell, M., Scott, D., et al. (2011). Fluorescence characteristics and sources of dissolved organic matter for stream water during storm events in a forested mid-Atlantic watershed. *Journal of Geophysical Research*, *116*(G3), G03043. https://doi.org/10.1029/2011JG001735

Jaffé, R., Cawley, K. M., & Yamashita, Y. (2014). Applications of excitation emission matrix fluorescence with parallel factor analysis (EEM-PARAFAC) in assessing environmental dynamics of natural dissolved organic matter (DOM) in aquatic environments: A review. In *Advances in the physicochemical characterization of dissolved organic matter: Impact on natural and engineered systems* (Vol. 1160, pp. 27–73). American Chemical Society. https://doi.org/10.1021/bk-2014-1160.ch003

Kaiser, K., Benner, R., & Amon, R. M. W. (2017). The fate of terrigenous dissolved organic carbon on the Eurasian shelves and export to the North Atlantic. *Journal of Geophysical Research: Oceans*, *122*(1), 4–22. https://doi.org/10.1002/2016JC012380

Kang, P.-G., & Mitchell, M. J. (2013). Bioavailability and size-fraction of dissolved organic carbon, nitrogen, and sulfur at the Arbutus Lake watershed, Adirondack Mountains, NY. *Biogeochemistry*, *115*(1), 213–234. https://doi.org/10.1007/s10533-013-9829-1

Kida, M., Fujitake, N., Suchewaboripont, V., Poungparn, S., Tomotsune, M., Kondo, M., et al. (2018). Contribution of humic substances to dissolved organic matter optical properties and iron mobilization. *Aquatic Sciences*, *80*(3), 26. https://doi.org/10.1007/s00027-018-0578-z

Kieber, R. J., Hydro, L. H., & Seaton, P. J. (1997). Photooxidation of triglycerides and fatty acids in seawater: Implication toward the formation of marine humic substances. *Limnology and Oceanography*, *42*(6), 1454–1462. https://doi.org/10.4319/lo.1997.42.6.1454

Kothawala, D. N., von Wachenfeldt, E., Koehler, B., & Tranvik, L. J. (2012). Selective loss and preservation of lake water dissolved organic matter fluorescence during long-term dark incubations. *Science of the Total Environment*, *433*, 238–246. https://doi.org/10.1016/j.scitotenv.2012.06.029

Kowalczuk, P., Tilstone, G. H., Zabłocka, M., Röttgers, R., & Thomas, R. (2013). Composition of dissolved organic matter along an Atlantic Meridional Transect from fluorescence spectroscopy and Parallel Factor Analysis. *Marine Chemistry*, *157*, 170–184. https://doi.org/10.1016/j.marchem.2013.10.004

Lamb, A. L., Wilson, G. P., & Leng, M. J. (2006). A review of coastal palaeoclimate and relative sea-level reconstructions using $\delta^{13}C$ and C/N ratios in organic material. *Earth-Science Reviews*, *75*(1), 29–57. https://doi.org/10.1016/j.earscirev.2005.10.003

Lawaetz, A. J., & Stedmon, C. A. (2009). Fluorescence intensity calibration using the Raman scatter peak of water. *Applied Spectroscopy*, *63*(8), 936–940. https://doi.org/10.1366/000370209788964548

Lee, M.-H., Osburn, C. L., Shin, K.-H., & Hur, J. (2018). New insight into the applicability of spectroscopic indices for dissolved organic matter (DOM) source discrimination in aquatic systems affected by biogeochemical processes. *Water Research*, *147*, 164–176. https://doi.org/10.1016/j.watres.2018.09.048

Lee, S. A., Kim, T. H., & Kim, G. (2020). Tracing terrestrial versus marine sources of dissolved organic carbon in a coastal bay using stable carbon isotopes. *Biogeosciences*, *17*(1), 135–144. https://doi.org/10.5194/bg-17-135-2020

Letscher, R. T., Hansell, D. A., & Kadko, D. (2011). Rapid removal of terrigenous dissolved organic carbon over the Eurasian shelves of the Arctic Ocean. *Marine Chemistry*, *123*(1), 78–87. https://doi.org/10.1016/j.marchem.2010.10.002

Lønborg, C., Álvarez-Salgado, X. A., Davidson, K., Martínez-García, S., & Teira, E. (2010). Assessing the microbial bioavailability and degradation rate constants of dissolved organic matter by fluorescence spectroscopy in the coastal upwelling system of the Ría de Vigo. *Marine Chemistry*, *119*(1), 121–129. https://doi.org/10.1016/j.marchem.2010.02.001

Louchouarn, P., Opsahl, S., & Benner, R. (2000). Isolation and quantification of dissolved lignin from natural waters using solid-phase extraction and GC/MS. *Analytical Chemistry*, *72*(13), 2780–2787. https://doi.org/10.1021/ac9912552

Lu, C.-J., Benner, R., Fichot, C. G., Fukuda, H., Yamashita, Y., & Ogawa, H. (2016). Sources and transformations of dissolved lignin phenols and chromophoric dissolved organic matter in Otsuchi Bay, Japan [Original Research]. *Frontiers in Marine Science*, *3*, 85. https://doi.org/10.3389/fmars.2016.00085

Magyan, S., & Dempsey, C. M. (2021). The role of time and mixing in the degradation of terrestrial derived dissolved organic carbon in lakes of varying trophic status. *Journal of Photochemistry and Photobiology*, *8*, 100065. https://doi.org/10.1016/j.jpap.2021.100065

Mann, P. J., Spencer, R. G. M., Hernes, P. J., Six, J., Aiken, G. R., Tank, S. E., et al. (2016). Pan-Arctic trends in terrestrial dissolved organic matter from optical measurements [Original Research]. *Frontiers in Earth Science*, *4*, 25. https://doi.org/10.3389/feart.2016.00025

Martin, P., Cherukuru, N., Tan, A. S. Y., Sanwlani, N., Mujahid, A., & Müller, M. (2018). Distribution and cycling of terrigenous dissolved organic carbon in peatland-draining rivers and coastal waters of Sarawak, Borneo. *Biogeosciences*, *15*(22), 6847–6865. https://doi.org/10.5194/bg-15-6847-2018

Martin, P., Moynihan, M. A., Chen, S., Woo, O. Y., Zhou, Y., Nichols, R. S., et al. (2022). Monsoon-driven biogeochemical dynamics in an equatorial shelf sea: Time-series observations in the Singapore Strait. *Estuarine, Coastal and Shelf Science*, *270*, 107855. https://doi.org/10.1016/j.ecss.2022.107855

Martin, P., Sanwlani, N., Lee, T. W. Q., Wong, J., Chang, K., Wong, E., & Liew, S. (2021). Dissolved organic matter from tropical peatlands reduces shelf sea light availability in the Singapore Strait, Southeast Asia. *Marine Ecology Progress Series*, *672*, 89–109. https://doi.org/10.3354/meps13776

Massicotte, P., Asmala, E., Stedmon, C., & Markager, S. (2017). Global distribution of dissolved organic matter along the aquatic continuum: Across rivers, lakes and oceans. *Science of the Total Environment*, *609*, 180–191. https://doi.org/10.1016/j.scitotenv.2017.07.076

Mayer, B., Siegel, H., Gerth, M., Pohlmann, T., Stottmeister, I., Putri, M., et al. (2022). 2 - Physical environment of the Indonesian Seas with focus on the western region. In T. C. Jennerjahn, T. Rixen, H. E. Irianto, & J. Samiaji (Eds.), *Science for the Protection of Indonesian Coastal Ecosystems (SPICE)* (pp. 13–43). Elsevier. https://doi.org/10.1016/B978-0-12-815050-4.00007-9

McKnight, D. M., Boyer, E. W., Westerhoff, P. K., Doran, P. T., Kulbe, T., & Andersen, D. T. (2001). Spectrofluorometric characterization of dissolved organic matter for indication of precursor organic material and aromaticity. *Limnology and Oceanography*, *46*(1), 38–48. https://doi.org/10.4319/lo.2001.46.1.0038

Medeiros, P. M., Seidel, M., Niggemann, J., Spencer, R. G. M., Hernes, P. J., Yager, P. L., et al. (2016). A novel molecular approach for tracing terrigenous dissolved organic matter into the deep ocean. *Global Biogeochemical Cycles*, *30*(5), 689–699. https://doi.org/10.1002/2015GB005320

Meyers-Schulte, K. J., & Hedges, J. I. (1986). Molecular evidence for a terrestrial component of organic matter dissolved in ocean water. *Nature*, *321*(6065), 61–63. https://doi.org/10.1038/321061a0

Miller, W. L., & Moran, M. A. (1997). Interaction of photochemical and microbial processes in the degradation of refractory dissolved organic matter from a coastal marine environment. *Limnology and Oceanography*, *42*(6), 1317–1324. https://doi.org/10.4319/lo.1997.42.6.1317

Mizubayashi, K., Kuwahara, V. S., Segaran, T. C., Zaleha, K., Effendy, A., Kushairi, M., & Toda, T. (2013). Monsoon variability of ultraviolet radiation (UVR) attenuation and bio-optical factors in the Asian tropical coral-reef waters. *Estuarine, Coastal and Shelf Science*, *126*, 34–43. https://doi.org/10.1016/j.ecss.2013.04.002

Moore, S., Gauci, V., Evans, C. D., & Page, S. E. (2011). Fluvial organic carbon losses from a Bornean blackwater river. *Biogeosciences*, *8*(4), 901–909. https://doi.org/10.5194/bg-8-901-2011

Moran, M. A., Sheldon, W. M., Jr., & Zepp, R. G. (2000). Carbon loss and optical property changes during long-term photochemical and biological degradation of estuarine dissolved organic matter. *Limnology and Oceanography*, *45*(6), 1254–1264. https://doi.org/10.4319/lo.2000.45.6.1254

Müller, D., Warneke, T., Rixen, T., Müller, M., Jamahari, S., Denis, N., et al. (2015). Lateral carbon fluxes and CO_2 outgassing from a tropical peat-draining river. *Biogeosciences*, *12*(20), 5967–5979. https://doi.org/10.5194/bg-12-5967-2015

Murphy, K. R., Stedmon, C. A., Graeber, D., & Bro, R. (2013). Fluorescence spectroscopy and multi-way techniques. PARAFAC. *Analytical Methods*, *5*(23), 6557–6566. https://doi.org/10.1039/C3AY41160E

Murphy, K. R., Stedmon, C. A., Waite, T. D., & Ruiz, G. M. (2008). Distinguishing between terrestrial and autochthonous organic matter sources in marine environments using fluorescence spectroscopy. *Marine Chemistry*, *108*(1), 40–58. https://doi.org/10.1016/j.marchem.2007.10.003

Murphy, K. R., Stedmon, C. A., Wenig, P., & Bro, R. (2014). OpenFluor– an online spectral library of auto-fluorescence by organic compounds in the environment. *Analytical Methods*, *6*(3), 658–661. https://doi.org/10.1039/C3AY41935E

Nichols, R. S., & Martin, P. (2021). Low biodegradability of dissolved organic matter from Southeast Asian peat-draining rivers. *Journal of Geophysical Research: Biogeosciences*, *126*(6), e2020JG006182. https://doi.org/10.1029/2020JG006182

Ohno, T. (2002). Fluorescence inner-filtering correction for determining the humification index of dissolved organic matter. *Environmental Science & Technology*, *36*(4), 742–746. https://doi.org/10.1021/es0155276

Opsahl, S., & Benner, R. (1997). Distribution and cycling of terrigenous dissolved organic matter in the ocean. *Nature*, *386*(6624), 480–482. https://doi.org/10.1038/386480a0

Opsahl, S., & Benner, R. (1998). Photochemical reactivity of dissolved lignin in river and ocean waters. *Limnology and Oceanography*, *43*(6), 1297–1304. https://doi.org/10.4319/lo.1998.43.6.1297

Opsahl, S. P., & Zepp, R. G. (2001). Photochemically-induced alteration of stable carbon isotope ratios ($\delta^{13}C$) in terrigenous dissolved organic carbon. *Geophysical Research Letters*, *28*(12), 2417–2420. https://doi.org/10.1029/2000gl012686

Ortega-Retuerta, E., Reche, I., Pulido-Villena, E., Agustí, S., & Duarte, C. (2010). Distribution and photoreactivity of chromophoric dissolved organic matter in the Antarctic Peninsula (Southern Ocean). *Marine Chemistry*, *118*(3), 129–139. https://doi.org/10.1016/j.marchem.2009.11.008

Osburn, C. L., Boyd, T. J., Montgomery, M. T., Bianchi, T. S., Coffin, R. B., & Paerl, H. W. (2016). Optical proxies for terrestrial dissolved organic matter in estuaries and coastal waters [Original Research]. *Frontiers in Marine Science*, *2*, 127. https://doi.org/10.3389/fmars.2015.00127

Osburn, C. L., Morris, D. P., Thorn, K. A., & Moeller, R. E. (2001). Chemical and optical changes in freshwater dissolved organic matter exposed to solar radiation. *Biogeochemistry*, *54*(3), 251–278. https://doi.org/10.1023/A:1010657428418

Osburn, C. L., Retamal, L., & Vincent, W. F. (2009). Photoreactivity of chromophoric dissolved organic matter transported by the Mackenzie River to the Beaufort Sea. *Marine Chemistry*, *115*(1), 10–20. https://doi.org/10.1016/j.marchem.2009.05.003

Osburn, C. L., & Stedmon, C. A. (2011). Linking the chemical and optical properties of dissolved organic matter in the Baltic–North Sea transition zone to differentiate three allochthonous inputs. *Marine Chemistry*, *126*(1), 281–294. https://doi.org/10.1016/j.marchem.2011.06.007

Painter, S. C., Lapworth, D. J., Woodward, E. M. S., Kroeger, S., Evans, C. D., Mayor, D. J., & Sanders, R. J. (2018). Terrestrial dissolved organic matter distribution in the North Sea. *Science of the Total Environment*, *630*, 630–647. https://doi.org/10.1016/j.scitotenv.2018.02.237

Qualls, R. G., & Richardson, C. J. (2003). Factors controlling concentration, export, and decomposition of dissolved organic nutrients in the Everglades of Florida. *Biogeochemistry*, *62*(2), 197–229. https://doi.org/10.1023/A:1021150503664

Raymond, P. A., & Spencer, R. G. M. (2015). Chapter 11 - Riverine DOM. In D. A. Hansell & C. A. Carlson (Eds.), *Biogeochemistry of marine dissolved organic matter* (2nd ed., pp. 509–533). Academic Press. https://doi.org/10.1016/B978-0-12-405940-5.00011-X

Reader, H. E., & Miller, W. L. (2012). Variability of carbon monoxide and carbon dioxide apparent quantum yield spectra in three coastal estuaries of the South Atlantic Bight. *Biogeosciences*, *9*(11), 4279–4294. https://doi.org/10.5194/bg-9-4279-2012

Rixen, T., Baum, A., Pohlmann, T., Balzer, W., Samiaji, J., & Jose, C. (2008). The Siak, a tropical black water river in central Sumatra on the verge of anoxia. *Biogeochemistry*, *90*(2), 129–140. https://doi.org/10.1007/s10533-008-9239-y

Rixen, T., Wit, F., Hutahaean, A. A., Schlüter, A., Baum, A., Klemme, A., et al. (2022). 4 - Carbon cycle in tropical peatlands and coastal seas. In T. C. Jennerjahn, T. Rixen, H. E. Irianto, & J. Samiaji (Eds.), *Science for the Protection of Indonesian Coastal Ecosystems (SPICE)* (pp. 83–142). Elsevier. https://doi.org/10.1016/B978-0-12-815050-4.00011-0

Samanta, S., Dalai, T. K., Pattanaik, J. K., Rai, S. K., & Mazumdar, A. (2015). Dissolved inorganic carbon (DIC) and its $\delta^{13}C$ in the Ganga (Hooghly) River estuary, India: Evidence of DIC generation via organic carbon degradation and carbonate dissolution. *Geochimica et Cosmochimica Acta*, *165*, 226–248. https://doi.org/10.1016/j.gca.2015.05.040

Sankar, M. S., Dash, P., Singh, S., Lu, Y., Mercer, A. E., & Chen, S. (2019). Effect of photo-biodegradation and biodegradation on the biogeochemical cycling of dissolved organic matter across diverse surface water bodies. *Journal of Environmental Sciences*, *77*, 130–147. https://doi.org/10.1016/j.jes.2018.06.021

Santos, L., Pinto, A., Filipe, O., Cunha, Â., Santos, E. B. H., & Almeida, A. (2016). Insights on the optical properties of estuarine DOM - Hydrological and biological influences. *PLoS One*, *11*(5), e0154519. https://doi.org/10.1371/journal.pone.0154519

Schmitt-Kopplin, P., Hertkorn, N., Schulten, H.-R., & Kettrup, A. (1998). Structural changes in a dissolved soil humic acid during photochemical degradation processes under O_2 and N_2 atmosphere. *Environmental Science & Technology*, *32*(17), 2531–2541. https://doi.org/10.1021/es970636z

Semiletov, I., Pipko, I., Gustafsson, Ö., Anderson, L. G., Sergienko, V., Pugach, S., et al. (2016). Acidification of East Siberian Arctic Shelf waters through addition of freshwater and terrestrial carbon. *Nature Geoscience*, *9*(5), 361–365. https://doi.org/10.1038/ngeo2695

Sharpless, C. M., & Blough, N. V. (2014). The importance of charge-transfer interactions in determining chromophoric dissolved organic matter (CDOM) optical and photochemical properties. *Environmental Science: Processes & Impacts*, *16*(4), 654–671. https://doi.org/10.1039/C3EM00573A

Siegel, H., Gerth, M., Stottmeister, I., et al. (2019). Remote sensing of coastal discharge of SE Sumatra (Indonesia). In V. Barale & M. Gade (Eds.), *Remote sensing of the Asian Seas* (pp. 359–376). Springer International Publishing. https://doi.org/10.1007/978-3-319-94067-0_20

Siegel, H., Stottmeister, I., Reißmann, J., Gerth, M., Jose, C., & Samiaji, J. (2009). Siak River System — East-Sumatra: Characterisation of sources, estuarine processes, and discharge into the Malacca Strait. *Journal of Marine Systems*, *77*(1), 148–159. https://doi.org/10.1016/j.jmarsys.2008.12.003

Spencer, R. G. M., Aiken, G. R., Butler, K. D., Dornblaser, M. M., Striegl, R. G., & Hernes, P. J. (2009). Utilizing chromophoric dissolved organic matter measurements to derive export and reactivity of dissolved organic carbon exported to the Arctic Ocean: A case study of the Yukon River, Alaska. *Geophysical Research Letters*, *36*(6), L06401. https://doi.org/10.1029/2008GL036831

Spencer, R. G. M., Butler, K. D., & Aiken, G. R. (2012). Dissolved organic carbon and chromophoric dissolved organic matter properties of rivers in the USA. *Journal of Geophysical Research*, *117*(G3), n/a. https://doi.org/10.1029/2011jg001928

Spencer, R. G. M., Hernes, P. J., Ruf, R., Baker, A., Dyda, R. Y., Stubbins, A., & Six, J. (2010). Temporal controls on dissolved organic matter and lignin biogeochemistry in a pristine tropical river, Democratic Republic of Congo. *Journal of Geophysical Research*, *115*(G3), G03013. https://doi.org/10.1029/2009JG001180

Spencer, R. G. M., Stubbins, A., Hernes, P. J., Baker, A., Mopper, K., Aufdenkampe, A. K., et al. (2009). Photochemical degradation of dissolved organic matter and dissolved lignin phenols from the Congo River. *Journal of Geophysical Research*, *114*(G3), G03010. https://doi.org/10.1029/2009JG000968

Stedmon, C. A., Amon, R. M. W., Rinehart, A. J., & Walker, S. (2011). The supply and characteristics of colored dissolved organic matter (CDOM) in the Arctic Ocean: Pan Arctic trends and differences. *Marine Chemistry*, *124*(1), 108–118. https://doi.org/10.1016/j.marchem.2010.12.007

Stedmon, C. A., & Bro, R. (2008). Characterizing dissolved organic matter fluorescence with parallel factor analysis: A tutorial. *Limnology and Oceanography: Methods*, *6*(11), 572–579. https://doi.org/10.4319/lom.2008.6.572

Stedmon, C. A., & Markager, S. (2005a). Resolving the variability in dissolved organic matter fluorescence in a temperate estuary and its catchment using PARAFAC analysis. *Limnology and Oceanography*, *50*(2), 686–697. https://doi.org/10.4319/lo.2005.50.2.0686

Stedmon, C. A., & Markager, S. (2005b). Tracing the production and degradation of autochthonous fractions of dissolved organic matter by fluorescence analysis. *Limnology and Oceanography*, *50*(5), 1415–1426. https://doi.org/10.4319/lo.2005.50.5.1415

Stedmon, C. A., Markager, S., & Bro, R. (2003). Tracing dissolved organic matter in aquatic environments using a new approach to fluorescence spectroscopy. *Marine Chemistry*, *82*(3), 239–254. https://doi.org/10.1016/S0304-4203(03)00072-0

Stedmon, C. A., & Nelson, N. B. (2015). Chapter 10 - The optical properties of DOM in the ocean. In D. A. Hansell & C. A. Carlson (Eds.), *Biogeochemistry of marine dissolved organic matter* (2nd ed., pp. 481–508). Academic Press. https://doi.org/10.1016/B978-0-12-405940-5.00010-8

Su, J., Cai, W.-J., Brodeur, J., Hussain, N., Chen, B., Testa, J. M., et al. (2020). Source partitioning of oxygen-consuming organic matter in the hypoxic zone of the Chesapeake Bay. *Limnology and Oceanography*, *65*(8), 1801–1817. https://doi.org/10.1002/lno.11419

Su, J., Dai, M., He, B., Wang, L., Gan, J., Guo, X., et al. (2017). Tracing the origin of the oxygen-consuming organic matter in the hypoxic zone in a large eutrophic estuary: The lower reach of the Pearl River Estuary, China. *Biogeosciences*, *14*(18), 4085–4099. https://doi.org/10.5194/bg-14-4085-2017

Susanto, R. D., Wei, Z., Adi, T. R., Zhang, Q., Fang, G., Fan, B., et al. (2016). Oceanography surrounding Krakatau Volcano in the Sunda Strait, Indonesia. *Oceanography*, *29*(2), 264–272. https://doi.org/10.5670/oceanog.2016.31

Urtizberea, A., Dupont, N., Rosland, R., & Aksnes, D. L. (2013). Sensitivity of euphotic zone properties to CDOM variations in marine ecosystem models. *Ecological Modelling*, *256*, 16–22. https://doi.org/10.1016/j.ecolmodel.2013.02.010

Vähätalo, A. V., & Zepp, R. G. (2005). Photochemical mineralization of dissolved organic nitrogen to ammonium in the Baltic Sea. *Environmental Science & Technology*, *39*(18), 6985–6992. https://doi.org/10.1021/es050142z

van Maren, D. S., & Gerritsen, H. (2012). Residual flow and tidal asymmetry in the Singapore Strait, with implications for resuspension and residual transport of sediment. *Journal of Geophysical Research*, *117*(C4), C04021. https://doi.org/10.1029/2011JC007615

Vantrepotte, V., Danhiez, F.-P., Loisel, H., Ouillon, S., Mériaux, X., Cauvin, A., & Dessailly, D. (2015). CDOM-DOC relationship in contrasted coastal waters: Implication for DOC retrieval from ocean color remote sensing observation. *Optics Express*, *23*(1), 33–54. https://doi.org/10.1364/OE.23.000033

Vione, D., Lauri, V., Minero, C., Maurino, V., Malandrino, M., Carlotti, M. E., et al. (2009). Photostability and photolability of dissolved organic matter upon irradiation of natural water samples under simulated sunlight. *Aquatic Sciences*, *71*(1), 34–45. https://doi.org/10.1007/s00027-008-8084-3

Walker, S. A., Amon, R. M. W., & Stedmon, C. A. (2013). Variations in high-latitude riverine fluorescent dissolved organic matter: A comparison of large Arctic rivers. *Journal of Geophysical Research: Biogeosciences*, *118*(4), 1689–1702. https://doi.org/10.1002/2013JG002320

Ward, C. P., Nalven, S. G., Crump, B. C., Kling, G. W., & Cory, R. M. (2017). Photochemical alteration of organic carbon draining permafrost soils shifts microbial metabolic pathways and stimulates respiration. *Nature Communications*, *8*(1), 772. https://doi.org/10.1038/s41467-017-00759-2

Weishaar, J. L., Aiken, G. R., Bergamaschi, B. A., Fram, M. S., Fujii, R., & Mopper, K. (2003). Evaluation of specific ultraviolet absorbance as an indicator of the chemical composition and reactivity of dissolved organic carbon. *Environmental Science & Technology*, *37*(20), 4702–4708. https://doi.org/10.1021/es030360x

Wilske, C., Herzsprung, P., Lechtenfeld, O. J., Kamjunke, N., & von Tümpling, W. (2020). Photochemically induced changes of dissolved organic natter in a humic-rich and forested stream. *Water*, *12*(2), 331. https://doi.org/10.3390/w12020331

Wit, F., Müller, D., Baum, A., Warneke, T., Pranowo, W. S., Müller, M., & Rixen, T. (2015). The impact of disturbed peatlands on river outgassing in Southeast Asia. *Nature Communications*, *6*(1), 10155. https://doi.org/10.1038/ncomms10155

Wit, F., Rixen, T., Baum, A., Pranowo, W. S., & Hutahaean, A. A. (2018). The invisible carbon footprint as a hidden impact of peatland degradation inducing marine carbonate dissolution in Sumatra, Indonesia. *Scientific Reports*, *8*(1), 17403. https://doi.org/10.1038/s41598-018-35769-7

Yamashita, Y., Fichot, C. G., Shen, Y., Jaffé, R., & Benner, R. (2015). Linkages among fluorescent dissolved organic matter, dissolved amino acids and lignin-derived phenols in a river-influenced ocean margin [Original Research]. *Frontiers in Marine Science*, *2*, 92. https://doi.org/10.3389/fmars.2015.00092

Yamashita, Y., Jaffé, R., Maie, N., & Tanoue, E. (2008). Assessing the dynamics of dissolved organic matter (DOM) in coastal environments by excitation emission matrix fluorescence and parallel factor analysis (EEM-PARAFAC). *Limnology and Oceanography*, *53*(5), 1900–1908. https://doi.org/10.4319/lo.2008.53.5.1900

Yamashita, Y., & Tanoue, E. (2003). Chemical characterization of protein-like fluorophores in DOM in relation to aromatic amino acids. *Marine Chemistry*, *82*(3), 255–271. https://doi.org/10.1016/S0304-4203(03)00073-2

Yang, L., & Hur, J. (2014). Critical evaluation of spectroscopic indices for organic matter source tracing via end member mixing analysis based on two contrasting sources. *Water Research*, *59*, 80–89. https://doi.org/10.1016/j.watres.2014.04.018

Ye, F., Guo, W., Wei, G., & Jia, G. (2018). The sources and transformations of dissolved organic matter in the Pearl River Estuary, China, as revealed by stable isotopes. *Journal of Geophysical Research: Oceans*, *123*(9), 6893–6908. https://doi.org/10.1029/2018JC014004

Zeebe, R. E., & Wolf-Gladrow, D. (2001). *CO_2 in seawater: Equilibrium, kinetics, isotopes*. Gulf Professional Publishing.

Zhou, Y., Evans, C. D., Chen, Y., Chang, K. Y. W., & Martin, P. (2021). Extensive remineralization of peatland-derived dissolved organic carbon and ocean acidification in the Sunda Shelf Sea, Southeast Asia. *Journal of Geophysical Research: Oceans*, *126*(6), e2021JC017292. https://doi.org/10.1029/2021JC017292

Zhou, Y., Martin, P., & Müller, M. (2019). Composition and cycling of dissolved organic matter from tropical peatlands of coastal Sarawak, Borneo, revealed by fluorescence spectroscopy and parallel factor analysis. *Biogeosciences*, *16*(13), 2733–2749. https://doi.org/10.5194/bg-16-2733-2019

Zhou, Y., Müller, M., Cherukuru, N., & Martin, P. (2023). Quantifying photodegradation of peatland-derived dissolved organic carbon in the coastal ocean of Southeast Asia. *Journal of Geophysical Research: Oceans*, *128*(12), e2023JC019741. https://doi.org/10.1029/2023JC019741

Zhu, Z. Y., Oakes, J., Eyre, B., Hao, Y., Sia, E. S. A., Jiang, S., et al. (2020). The nonconservative distribution pattern of organic matter in the Rajang, a tropical river with peatland in its estuary. *Biogeosciences*, *17*(9), 2473–2485. https://doi.org/10.5194/bg-17-2473-2020

Zigah, P. K., McNichol, A. P., Xu, L., Johnson, C., Santinelli, C., Karl, D. M., & Repeta, D. J. (2017). Allochthonous sources and dynamic cycling of ocean dissolved organic carbon revealed by carbon isotopes. *Geophysical Research Letters*, *44*(5), 2407–2415. https://doi.org/10.1002/2016GL071348

Zsolnay, A., Baigar, E., Jimenez, M., Steinweg, B., & Saccomandi, F. (1999). Differentiating with fluorescence spectroscopy the sources of dissolved organic matter in soils subjected to drying. *Chemosphere*, *38*(1), 45–50. https://doi.org/10.1016/S0045-6535(98)00166-0

References From the Supporting Information

Rau, G. H., Riebesell, U., & Wolf-Gladrow, D. (1996). A model of photosynthetic ^{13}C fractionation by marine phytoplankton based on diffusive molecular CO_2 uptake. *Marine Ecology Progress Series*, *133*, 275–285. https://doi.org/10.3354/meps133275

Su, J., Cai, W.-J., Hussain, N., Brodeur, J., Chen, B., & Huang, K. (2019). Simultaneous determination of dissolved inorganic carbon (DIC) concentration and stable isotope ($\delta^{13}C$-DIC) by Cavity Ring-Down Spectroscopy: Application to study carbonate dynamics in the Chesapeake Bay. *Marine Chemistry*, *215*, 103689. https://doi.org/10.1016/j.marchem.2019.103689